

# Log-Concave Ridge Estimation\*

Christof Strähl  
University of Bern, Switzerland

November 7, 2021

## Abstract

We develop a density ridge search algorithm based on a novel density ridge definition. This definition is based on a conditional variance matrix and the mode in the lower dimensional subspace. It is compared to the subspace constraint mean shift algorithm in Ozertem and Erdogmus (2011), based on the gradient and Hessian of the underlying probability density function. We show the advantages of the new algorithm in a simulation study and estimate galaxy filaments from a data set of the Baryon Oscillation Spectroscopic Survey.

## Contents

<b>1</b>	<b>Introduction</b>	<b>2</b>
1.1	From Principle Curves to Ridges . . . . .	2
1.2	Ridge definitions. . . . .	3
<b>2</b>	<b>Algorithms</b>	<b>7</b>
2.1	Mean Shift Algorithm . . . . .	7
2.2	Subspace Constraint Mean Shift Algorithm . . . . .	8
2.3	Log-Concave Ridge Search Algorithm . . . . .	9
<b>3</b>	<b>Data Examples</b>	<b>14</b>
3.1	Circle Data . . . . .	14
3.2	Galaxy filaments . . . . .	15
3.3	Discussion . . . . .	20

---

\*This work was supported by Swiss National Science Foundation. It is part of the author's PhD dissertation.

<b>A Auxiliary Results</b>	<b>22</b>
A.1 Ridge of circle data . . . . .	22
A.2 Matrix Analysis . . . . .	24
<b>B Proofs</b>	<b>24</b>
B.1 Ridges . . . . .	24
B.2 Algorithms . . . . .	26

# 1 Introduction

## 1.1 From Principle Curves to Ridges

Nowadays, a ridge of a probability distribution is understood as a lower dimensional structure, where each point on the ridge is the mode in an affine subspace. The subspace is given by some eigenvectors of the Hessian of the underlying probability density function; see Ozertem and Erdogmus (2011), Genovese et al. (2014). We give a more general definition, where the subspace is given by the directions with smallest local variance.

An early approach to define lower dimensional structures of a distribution were made by Hastie and Stuetzle (1989). In their paper, a principle curve is a smooth curve through the middle of the data. For any point on the curve the average of all data points coincides with the point. More formally, they give a definition for principle curves of probability density functions as follows:

**Definition 1.1.** Let  $f$  be a probability density function on  $\mathbb{R}^d$  with corresponding random vector  $\mathbf{X}$  with finite second moments and assume without loss of generality that  $\mathbb{E}(\mathbf{X}) = 0$ . Let  $\gamma$  be a differentiable unit-speed curve in  $\mathbb{R}^d$  parameterized over  $I \subset \mathbb{R}$ , i.e.  $\|\gamma'(t)\| = 1$  for  $t \in I$ , that does not intersect itself and has finite length inside any finite ball in  $\mathbb{R}^d$ . Define the *projection index*  $t_\gamma : \mathbb{R}^d \rightarrow \mathbb{R}$  as

$$t_\gamma(\mathbf{x}) = \sup_t \{t : \|\mathbf{x} - \gamma(t)\| = \inf_s \|\mathbf{x} - \gamma(s)\|\}.$$

The curve  $\gamma$  is called *self-consistent* or a *principle curve* of  $f$  if  $\mathbb{E}(\mathbf{X} | t_\gamma(\mathbf{X}) = t) = \gamma(t)$  for a.e.  $t$ .

The intuition behind the principle curves in Definition 1.1 is that for any parameter value  $t$  we collect the points projected on  $\gamma(t)$  on the principle curve, and their average should lie on the principle curve. A distribution may have multiple principle curves, i.e. for any spherically symmetric distribution any straight line through the center is a principle curve. The existence of principal curves remains an open question, expect for very special cases, i.e. elliptical distributions.

Kégl et al. (2000) address the issue in Hastie and Stuetzle (1989), that principle curves do not exist for any distribution. To resolve this problem they generalize a property of principle components: A straight line  $\gamma(t)$  is the first principle component, if and only if,

$$\mathbb{E}(\min_t \|\mathbf{X} - \gamma(t)\|^2) \leq \mathbb{E}(\min_t \|\mathbf{X} - \hat{\gamma}(t)\|^2)$$

for any other straight line  $\hat{\gamma}$ . Instead of considering straight lines only, they restrict the class of curves on those with finite length. The finite length constraint is necessary, because otherwise the expected squared

distance between  $\mathbf{X}$  and the curve becomes arbitrary small and the length of the curve tends to infinity. The formal definition of a principle curve is the following:

**Definition 1.2.** A curve  $\gamma$  is called *principal curve of length  $L$  for  $\mathbf{X}$*  if  $\gamma$  minimizes

$$\Delta(\gamma) := \mathbb{E}(\inf_t \|\mathbf{X} - \gamma(t)\|^2) = \mathbb{E}(\|\mathbf{X} - \gamma(t_\gamma(\mathbf{X}))\|^2)$$

over all curves of length less than or equal to  $L$ .

Whenever  $\mathbf{X}$  has finite second moments, a principle curve as in Definition 1.2 exists. They present the polygonal line algorithm to estimate the principle curve.

In Delicado (2001) and Delicado and Huerta (2003), a principle curve (of oriented points) is defined as a curve contained in the set of oriented points. A point  $\mathbf{x}$  is oriented, whenever it holds  $\mathbf{x} = \mathbb{E}(\mathbf{X} | \mathbf{X} \in H(\mathbf{x}, \mathbf{b}))$ , where  $\mathbf{b}$  is the unit vector, such that the total variance  $\text{tr}(\text{Var}(\mathbf{X} | \mathbf{X} \in H(\mathbf{x}, \mathbf{b})))$  is minimal for the hyperplane  $H(\mathbf{x}, \mathbf{b}) := \{\mathbf{y} \in \mathbb{R}^d : (\mathbf{y} - \mathbf{x})^\top \mathbf{b} = 0\}$ . That means, the principle curve consists of averages of  $\mathbf{X}$ , given  $\mathbf{X}$  lies in a hyperplane orthogonal to the direction with largest variance.

All the concepts so far only consider one-dimensional structures. Furthermore, they are based on the expectation and not on the shape of the underlying density function.

This changes with Ozertem and Erdogmus (2011). Their definition of a principle curve is based on the gradient and Hessian matrix of the underlying probability density function. They also generalize the definition from one-dimensional curves to arbitrary lower dimensional structures, called principle sets. Because the ridge definition in Genovese et al. (2014) is very similar to the one of principle curves and sets in Ozertem and Erdogmus (2011), we will not state it here. The differences are discussed after Definition 1.4.

A ridge as defined in Genovese et al. (2014) is a  $s$ -dimensional structure containing all points, where the  $s$  smallest eigenvalues of the Hessian matrix are negative, and the corresponding eigenvectors are orthogonal to the gradient; see Definition 1.4. This means, each point in the ridge is a mode in the affine subspace spanned by the eigenvectors corresponding to the  $s$  smallest eigenvalues of the Hessian.

In our ridge definition (Definition 1.3) we replace the Hessian matrix by a conditional covariance matrix and instead of relying on the gradient to check for a mode in the affine subspace, we just require that there is such a mode. Therefore, we can relax the conditions on the probability density function; see Definition 1.3. However, if the stronger conditions hold, both definitions are equivalent.

## 1.2 Ridge definitions.

**Density function.** We always assume that the density function  $f \in \mathcal{C}(\mathbb{R}^d)$ . To show the equivalence between both ridge definitions we assume further

(A1)  $f \in \mathcal{C}^2(\mathbb{R}^d)$  with positive eigengap

$$\delta(\mathbf{x}) := \lambda_s(D^2\ell(\mathbf{x})) - \lambda_{s+1}(D^2\ell(\mathbf{x})) > 0$$

for all  $\mathbf{x} \in \{f > 0\}$ , where  $\ell = \log f$ .

**The kernel function.** All algorithm involve a bounded kernel function  $K : \mathbb{R}^d \rightarrow [0, \infty)$  such that

$$(K0) \quad \int K(\mathbf{z}) d\mathbf{z} = 1.$$

(K1)  $K$  is sign- and permutation-symmetric, i.e.

$$K(z_1, z_2, \dots, z_d) = K(\xi_1 z_{\sigma(1)}, \xi_2 z_{\sigma(2)}, \dots, \xi_d z_{\sigma(d)})$$

for all  $\mathbf{z} \in \mathbb{R}^d$ ,  $\boldsymbol{\xi} \in \{-1, 1\}^d$  and  $\sigma \in \mathcal{S}_d$ , the set of permutations on  $\{1, 2, \dots, d\}$ .

(K2)  $\int K(\mathbf{z}) \mathbf{z} \mathbf{z}^\top = \mathbf{I}_d$ , the identity matrix in  $\mathbb{R}^d$ .

To get equivalence between both ridge definitions or to apply the algorithms presented later, we will require additional conditions.

(K3) It holds

$$\mu_4 := \int K(\mathbf{z}) z_1^4 d\mathbf{z} = 3 \quad \text{and} \quad \mu_{22} := \int K(\mathbf{z}) z_1^2 z_2^2 d\mathbf{z} = 1.$$

(K4)  $K$  is rotationally symmetric, i.e. there exists a *profile* of the kernel  $k : \mathbb{R} \rightarrow [0, \infty)$  such that  $K(\mathbf{z}) = c_{k,d} k(\|\mathbf{z}\|^2)$  for some constant  $c_{k,d}$ .

(K5) The kernel  $K$  is log-concave and  $K \in \mathcal{C}_b^2(\mathbb{R}^d)$ , this means, all partial derivatives of order 2 exist and are bounded. Moreover, the largest eigenvalue of  $D^2 \log K$  is negative and bounded away from 0.

For our definitions and algorithms we need rescaled versions of  $K$ . For any bandwidth  $h > 0$  we write

$$K_h(\mathbf{z}) := h^{-d} K(h^{-1} \mathbf{z}).$$

A particular choice of  $K$  fulfilling (K0–5) is the standard Gaussian density

$$\mathbf{z} \mapsto (2\pi)^{-d/2} \exp(-|\mathbf{z}|^2/2).$$

**Two density ridge definitions.** Both definitions and algorithms involve the spectral decomposition of either the Hessian matrix of  $f$  or  $\ell$ , or the conditional covariance matrix.

For a symmetric matrix  $\mathbf{M} \in \mathbb{R}^{d \times d}$  we denote the vector of eigenvalues in decreasing order by

$$\boldsymbol{\lambda}(\mathbf{M}) = (\lambda_1(\mathbf{M}), \lambda_2(\mathbf{M}), \dots, \lambda_d(\mathbf{M})) \quad \text{with} \quad \lambda_1(\mathbf{M}) \geq \lambda_2(\mathbf{M}) \geq \dots \geq \lambda_d(\mathbf{M}),$$

the matrix with the eigenvalues on the diagonal by  $\mathbf{\Lambda}(\mathbf{M}) = \text{diag}(\boldsymbol{\lambda}(\mathbf{M}))$  and the corresponding eigenvectors by

$$\mathbf{V}(\mathbf{M}) = [\mathbf{v}_1(\mathbf{M}), \mathbf{v}_2(\mathbf{M}), \dots, \mathbf{v}_d(\mathbf{M})], \quad \text{where} \quad \lambda_j(\mathbf{M}) \mathbf{v}_j(\mathbf{M}) = \mathbf{M} \mathbf{v}_j(\mathbf{M}) \quad \text{for} \quad 1 \leq j \leq d.$$

We are usually interested in the space spanned by the  $s$  largest or the  $d - s$  smallest eigenvalues. Hence we write for fixed  $1 \leq s < d$

$$\mathbf{V}_\parallel(\mathbf{M}) = [\mathbf{v}_1(\mathbf{M}), \dots, \mathbf{v}_s(\mathbf{M})] \quad \text{and} \quad \mathbf{V}_\perp(\mathbf{M}) = [\mathbf{v}_{s+1}(\mathbf{M}), \dots, \mathbf{v}_d(\mathbf{M})].$$

The matrix  $\mathbf{V}_\perp(\mathbf{M}) \mathbf{V}_\perp(\mathbf{M})^\top$  projects a vector onto the space spanned by  $\mathbf{v}_{s+1}(\mathbf{M}), \dots, \mathbf{v}_d(\mathbf{M})$ . The distance between two such subspaces generated by matrices  $\mathbf{A}, \mathbf{B} \in \mathbb{R}_{\text{sym}}^{d \times d}$  is defined by

$$\text{dist}(\mathbf{V}_\perp(\mathbf{A}), \mathbf{V}_\perp(\mathbf{B})) := \|\mathbf{V}_\perp(\mathbf{A}) \mathbf{V}_\perp(\mathbf{A})^\top - \mathbf{V}_\perp(\mathbf{B}) \mathbf{V}_\perp(\mathbf{B})^\top\|_F,$$

where  $\|\cdot\|_F$  denotes the Frobenius norm.

Next, we present a new ridge definition rely on fewer assumptions on the underlying density function, followed by the usual ridge definition given e.g in Eberly (1996), Genovese et al. (2014).

**Definition 1.3.** Suppose (K0–3) hold. Let  $\mathbf{X}$  and  $\mathbf{Z}_h$  be independent random vectors with density functions  $f$  and  $K_h$ , respectively. We define the *conditional covariance matrix*

$$\Sigma_h(\mathbf{x}) := \text{Var}(\mathbf{X} | \mathbf{X} + \mathbf{Z}_h = \mathbf{x}).$$

Assume there exists a matrix  $\mathbf{V}_\perp(\mathbf{x}) \in \mathbb{R}^{d \times (d-s)}$  with orthonormal columns, such that

$$\text{dist}(\mathbf{V}_\perp(\Sigma_h(\mathbf{x})), \mathbf{V}_\perp(\mathbf{x})) \rightarrow 0 \quad \text{as } h \rightarrow \infty \quad \text{for each } \mathbf{x} \in \{f > 0\}.$$

The  $s$ -dimensional ridge of  $f$  is then

$$R_s(f) := \{\mathbf{x} \in \mathbb{R}^d : \mathbb{R}^{d-s} \ni \mathbf{z} \mapsto f(\mathbf{x} + \mathbf{V}_\perp(\mathbf{x})\mathbf{z}) \text{ has a mode at } \mathbf{0}_{d-s}\}.$$

**Definition 1.4.** Let  $f \in \mathcal{C}^2(\mathbb{R}^d)$  be a probability density function with gradient  $\mathbf{g}(\mathbf{x})$  and Hessian matrix  $\mathbf{H}(\mathbf{x})$  at point  $\mathbf{x}$ . The ridge  $\tilde{R}_s(f)$  of  $f$  with dimension  $s$  is given by

$$\tilde{R}_s(f) = \{\mathbf{x} : \mathbf{V}_\perp(\mathbf{H}(\mathbf{x}))^\top \mathbf{g}(\mathbf{x}) = \mathbf{0}, \lambda_{s+1}(\mathbf{H}(\mathbf{x})) < 0\}.$$

Definition 1.4 is almost identical to the definition of principle sets in Ozertem and Erdogmus (2011). The only difference is in the inclusion or exclusion of points already contained in a lower dimensional ridge. In Definition 1.4 we have

$$\tilde{R}_0(f) \subset \tilde{R}_1(f) \subset \dots \subset \tilde{R}_{d-1}(f).$$

However, a principle set of dimension  $s$  is defined as  $\tilde{R}_0(f)$  for  $s = 0$  and  $\tilde{R}_s(f) \setminus \tilde{R}_{s-1}(f)$  for  $1 \leq s \leq d-1$ . Hence, in general, only the 0-dimensional principle sets and ridges coincide, which are the local maxima of the probability density function.

Ozertem and Erdogmus (2011) show that the principle sets, and hence the ridges, are the same for  $f$  and  $p \circ f$ , where  $p$  is a monotonically increasing function on  $\mathbb{R}$ . Especially, replacing the Hessian of  $f$  with the Hessian of  $\log \circ f$  in Definition 1.4 leads to the same ridge.

**Weighted distribution.** Let  $\mathbf{X}$  and  $\mathbf{Z}_h$  be independent with probability density  $f$  and  $K_h$ , respectively. Let  $q$  be the probability density of  $\mathbf{X}$ , given  $\mathbf{X} + \mathbf{Z}_h = \mathbf{x}$ , then

$$q(\mathbf{y}) = \frac{f_{\mathbf{X}, \mathbf{X} + \mathbf{Z}_h = \mathbf{x}}(\mathbf{y}, \mathbf{x})}{f_{\mathbf{X} + \mathbf{Z}_h}(\mathbf{x})} = \frac{f(\mathbf{y})K_h(\mathbf{y} - \mathbf{x})}{\int f(\mathbf{z})K_h(\mathbf{z} - \mathbf{x}) d\mathbf{z}} = s_h(\mathbf{x})^{-1}K_h(\mathbf{y} - \mathbf{x})f(\mathbf{y}),$$

where  $s_h(\mathbf{x}) := \int K(\mathbf{z})f(\mathbf{x} + h\mathbf{z}) d\mathbf{z}$ . Let the conditional expectation be

$$\begin{aligned} \boldsymbol{\mu}_h(\mathbf{x}) &:= \mathbb{E}(\mathbf{X} | \mathbf{X} + \mathbf{Z}_h = \mathbf{x}) \\ &= s_h(\mathbf{x})^{-1} \int K(\mathbf{z})(\mathbf{x} + h\mathbf{z})f(\mathbf{x} + h\mathbf{z}) d\mathbf{z} \\ &= \mathbf{x} + h s_h(\mathbf{x})^{-1} \mathbf{s}_h(\mathbf{x}), \end{aligned}$$

where  $\mathbf{s}_h(\mathbf{x}) := \int K(\mathbf{z})\mathbf{z}f(\mathbf{x} + h\mathbf{z}) d\mathbf{z}$  and the conditional variance

$$\begin{aligned} \Sigma_h(\mathbf{x}) &:= \text{Var}(\mathbf{X} | \mathbf{X} + \mathbf{Z}_h = \mathbf{x}) \\ &= \int \mathbf{y}\mathbf{y}^\top q(\mathbf{y}) d\mathbf{y} - \boldsymbol{\mu}_h(\mathbf{x})\boldsymbol{\mu}_h(\mathbf{x})^\top \\ &= h^2(s_h(\mathbf{x})^{-1}\mathbf{S}_h(\mathbf{x}) - s_h(\mathbf{x})^{-2}\mathbf{s}_h(\mathbf{x})\mathbf{s}_h(\mathbf{x})^\top), \end{aligned}$$

because

$$\begin{aligned} \int \mathbf{y} \mathbf{y}^\top f(\mathbf{y}) K_h(\mathbf{y} - \mathbf{x}) d\mathbf{y} &= \int (\mathbf{x} + h\mathbf{z})(\mathbf{x} + h\mathbf{z})^\top K(\mathbf{z}) f(\mathbf{x} + h\mathbf{z}) d\mathbf{z} \\ &= \mathbf{x} \mathbf{x}^\top s_h(\mathbf{x}) + h \mathbf{x} \mathbf{s}_h(\mathbf{x})^\top + h \mathbf{s}_h(\mathbf{x}) \mathbf{x}^\top + h^2 \mathbf{S}_h(\mathbf{x}), \end{aligned}$$

where  $\mathbf{S}_h(\mathbf{x}) := \int K(\mathbf{z}) \mathbf{z} \mathbf{z}^\top f(\mathbf{x} + h\mathbf{z}) d\mathbf{z}$ .

The following Lemma is a direct consequence of Corollary 2.2 in Strähl et al. (2020) about local moments.

**Lemma 1.5.** *Suppose  $f \in \mathcal{C}^2(\mathbb{R}^d)$  and conditions (K0–2) hold, then for  $\mathbf{x} \in \{f > 0\}$ ,*

$$\begin{aligned} \boldsymbol{\mu}_h(\mathbf{x}) &= \mathbf{x} + h^2 f(\mathbf{x})^{-1} Df(\mathbf{x}) + o(h^3), \\ \boldsymbol{\Sigma}_h(\mathbf{x}) &= h^2 \mathbf{I}_d + 2^{-1}(\mu_{22} - 1) h^4 f(\mathbf{x})^{-1} \text{tr}(D^2 f(\mathbf{x})) \mathbf{I}_d + h^4 f(\mathbf{x})^{-1} D^2 f(\mathbf{x}) \odot \mathbf{M} \\ &\quad - h^4 f(\mathbf{x})^{-2} Df(\mathbf{x}) Df(\mathbf{x})^\top + o(h^4) \end{aligned}$$

as  $h \rightarrow 0$ , locally uniformly in  $\mathbf{x}$ . Here  $\odot$  denotes the componentwise product of matrices, and  $\mathbf{M}$  is the matrix with entries  $M_{jk} := \mathbb{1}\{j = k\}(\mu_4 - \mu_{22})/2 + \mathbb{1}\{j \neq k\}\mu_{22}$  for  $j, k = 1, \dots, d$ . If the kernel function fulfills (K3), then

$$\boldsymbol{\Sigma}_h(\mathbf{x}) = h^2 \mathbf{I}_d + h^4 D^2 \log f(\mathbf{x}) + o(h^4) \quad \text{as } h \rightarrow 0, \text{ locally uniformly in } \mathbf{x}.$$

**Equivalence of the two ridge definitions.** Theorem 1.6 shows that under (A1) and (K0–3) the subspace generated by the conditional covariance matrix converges to the subspace generated by the Hessian of the log-density and Theorem 1.7 shows that under the same assumptions at any ridge point  $\mathbf{x} \in R_s(f)$ , the density function restricted to the subspace spanned by  $\mathbf{V}_\perp(D^2 f(\mathbf{x}))$  is log-concave with mode at  $\mathbf{0}_{d-s}$ . Together they imply  $\tilde{R}_s(f) \subset R_s(f)$ . Theorem 1.8 shows  $R_s(f) \subset \tilde{R}_s(f)$  again under the same conditions, and so  $\tilde{R}_s(f) = R_s(f)$ .

**Theorem 1.6.** *Suppose (A1) and (K0–2) hold, then*

$$\text{dist}(\mathbf{V}_\perp(\boldsymbol{\Sigma}_h(\mathbf{x})), \mathbf{V}_\perp(\mathbf{H}(\mathbf{x}))) \rightarrow 0 \quad \text{as } h \rightarrow 0.$$

**Theorem 1.7.** *Suppose (A1) and (K0–2) hold and  $\mathbf{x} \in \tilde{R}_s(f)$ ; see Definition 1.4. Then there exists  $\varepsilon > 0$ , such that the function*

$$\mathbf{z}'' \mapsto f(\mathbf{x} + \mathbf{V}_\perp(D^2 f(\mathbf{x})) \mathbf{z}'')$$

*is log-concave on  $\{\mathbf{z}'' \in \mathbb{R}^{d-s} : \|\mathbf{z}''\| < \varepsilon\}$  with a mode at  $\mathbf{0}_{d-s}$ . In particular,  $t \mapsto f(\mathbf{x} + t\mathbf{u})$  has a mode at 0 for any  $\mathbf{u}$  in the column space of  $\mathbf{V}_\perp(D^2 \ell(\mathbf{x}))$ .*

**Theorem 1.8.** *Suppose that (A1) and (K0–2) hold and  $\mathbf{x} \in R_s(f)$ ; see Definition 1.3. Then*

$$\mathbf{V}_\perp(D\ell(\mathbf{x}))^\top D\ell(\mathbf{x}) = \mathbf{0} \quad \text{and} \quad \lambda_{s+1}(D^2 \ell(\mathbf{x})) < 0.$$

**Projected weighted distribution.** Suppose  $f \in \mathcal{C}(\mathbb{R}^d)$  and the conditions (K0–4) hold. Let  $\mathbf{V} = [\mathbf{V}_\parallel, \mathbf{V}_\perp] \in \mathbb{R}^{d \times d}$  be a orthogonal matrix with  $\mathbf{V}_\parallel \in \mathbb{R}^{d \times s}$  and  $\mathbf{V}_\perp \in \mathbb{R}^{d \times (d-s)}$ . The probability density function of  $\mathbf{X} - \mathbf{x}$ , given  $\mathbf{X} + \mathbf{Z}_h = \mathbf{x}$ , is

$$\mathbf{y} \mapsto \frac{K_h(\mathbf{y}) f(\mathbf{y} + \mathbf{x})}{\int K_h(\mathbf{z}) f(\mathbf{z} + \mathbf{x}) d\mathbf{z}} = s_h(\mathbf{x})^{-1} K_h(\mathbf{y}) f(\mathbf{y} + \mathbf{x}).$$

Hence, the probability density function of the rotated distribution  $\mathbf{V}^\top(\mathbf{X} - \mathbf{x})$ , given  $\mathbf{X} + \mathbf{Z}_h = \mathbf{x}$ , is

$$\mathbf{y} \mapsto s_h(\mathbf{x})^{-1} |\det(\mathbf{V})|^{-1} K_h(\mathbf{V}^{-\top} \mathbf{y}) f(\mathbf{x} + \mathbf{V}^{-\top} \mathbf{y}) = s_h(\mathbf{x})^{-1} K_h(\mathbf{V} \mathbf{y}) f(\mathbf{x} + \mathbf{V} \mathbf{y}).$$

---

**Algorithm 1:** Mean Shift

---

**Data:**  $\mathbf{X}_1, \mathbf{X}_2, \dots, \mathbf{X}_n$   
**Input:** Starting point  $\mathbf{x}$ , bandwidth  $h > 0$ ,  $\text{tol} > 0$   
**Result:** Mode close to  $\mathbf{x}$   
**begin**  
     $\mathbf{m} \leftarrow \mathbf{m}_{h,G}(\mathbf{x})$   
    **while**  $\|\mathbf{m}\| > \text{tol}$  **do**  
         $\mathbf{x} \leftarrow \mathbf{x} + \mathbf{m}$   
         $\mathbf{m} \leftarrow \mathbf{m}_{h,G}(\mathbf{x})$   
    **return**  $\mathbf{x}$   

---

Finally, the probability density function of  $\mathbf{V}_\perp^\top(\mathbf{X} - \mathbf{x})$ , given  $\mathbf{X} + \mathbf{Z}_h = \mathbf{x}$ , is

$$\mathbf{y}'' \mapsto \mathbf{s}_h(\mathbf{x})^{-1} \int_{\mathbb{R}^s} K_h(\mathbf{y}) f(\mathbf{x} + \mathbf{V}\mathbf{y}) d\mathbf{y}',$$

where  $\mathbf{y} = (\mathbf{y}', \mathbf{y}'')$ . Note that  $K_h(\mathbf{V}\mathbf{y}) = K_h(\mathbf{y})$  by (K4). In the case of  $\mathbf{V}_\perp = \mathbf{V}_\perp(\boldsymbol{\Sigma}_h(\mathbf{x}))$  as in Definition 1.3, we define

$$g_h(\mathbf{z}'') := \mathbf{s}_h(\mathbf{x})^{-1} \int_{\mathbb{R}^s} K(\mathbf{z}) f(\mathbf{x} + h\mathbf{V}(\boldsymbol{\Sigma}_h(\mathbf{x}))\mathbf{z}) d\mathbf{z}',$$

the weighted density of  $f$  projected onto the  $(d-s)$ -dimensional space spanned by the directions of lowest conditional variance.

**Theorem 1.9.** *Suppose  $f = e^\ell$  with  $\ell \in \mathcal{C}^2(\mathbb{R}^d)$  and bounded second order partial derivatives. Suppose conditions (K0–5) hold and  $\mathbf{x} \in R_s(f)$ . Then there exists  $h_o > 0$  such that the projected weighted density  $g_h$  is log-concave for all  $0 < h \leq h_o$ .*

Theorem 1.9 justifies using a log-concave density estimator on the sample projected weighted distribution to estimate a point on the density ridge.

## 2 Algorithms

We consider independent random vectors  $\mathbf{X}_1, \mathbf{X}_2, \dots, \mathbf{X}_n$  with distribution given by the density function  $f : \mathbb{R}^d \rightarrow [0, \infty)$ . Our goal is to estimate the density ridge of  $f$ .

### 2.1 Mean Shift Algorithm

The mean shift algorithm is an iterative procedure to find the modes of a distribution; see Cheng (1995), Comaniciu et al. (2002). First, the density is estimated by kernel density estimation (KDE) with a rotationally symmetric kernel  $K$  as in (K4). An estimator for  $f$  and  $Df$  is then given by

$$\hat{f}_{h,K}(\mathbf{x}) = \frac{c_{k,d}}{nh^d} \sum_{i=1}^n k\left(\left\|\frac{\mathbf{X}_i - \mathbf{x}}{h}\right\|^2\right) \quad \text{and} \quad D\hat{f}_{h,K}(\mathbf{x}) = -\frac{2c_{k,d}}{nh^{d+2}} \sum_{i=1}^n (\mathbf{X}_i - \mathbf{x}) k'\left(\left\|\frac{\mathbf{X}_i - \mathbf{x}}{h}\right\|^2\right),$$

---

**Algorithm 2:** Subspace Constraint Mean Shift

---

**Data:**  $\mathbf{X}_1, \mathbf{X}_2, \dots, \mathbf{X}_n$   
**Input:** Starting point  $\mathbf{x}$ , bandwidth  $h > 0$ ,  $\text{tol} > 0$   
**Result:** Ridge point close to  $\mathbf{x}$   
**begin**  
     $\mathbf{m} \leftarrow \mathbf{m}_{h,G}(\mathbf{x})$   
     $\mathbf{g} \leftarrow D\hat{f}_{h,K}(\mathbf{x})$   
     $\mathbf{H} \leftarrow D^2 \log \hat{f}_{h,K}(\mathbf{x})$   
    **while**  $|\mathbf{g}^\top \mathbf{H} \mathbf{g}| > (1 - \text{tol}) \|\mathbf{g}\| \cdot \|\mathbf{H} \mathbf{g}\|$  **do**  
         $\mathbf{x} \leftarrow \mathbf{x} + \mathbf{V}_\perp(\mathbf{H}) \mathbf{V}_\perp(\mathbf{H})^\top \mathbf{m}$   
         $\mathbf{m} \leftarrow \mathbf{m}_{h,G}(\mathbf{x})$   
         $\mathbf{g} \leftarrow D\hat{f}_{h,K}(\mathbf{x})$   
         $\mathbf{H} \leftarrow D^2 \log \hat{f}_{h,K}(\mathbf{x})$   
    **return**  $\mathbf{y}$

---

respectively. By defining  $g(\mathbf{x}) = -k'(\mathbf{x})$  and  $G(\mathbf{x}) = c_{g,d}g(\|\mathbf{x}\|^2)$ , where  $c_{g,d}$  is the corresponding normalization constant, we can write

$$\begin{aligned} D\hat{f}_{h,K}(\mathbf{x}) &= \frac{2c_{k,d}}{nh^{d+2}} \left( \sum_{i=1}^n g\left(\left\|\frac{\mathbf{X}_i - \mathbf{x}}{h}\right\|^2\right) \right) \left( \frac{\sum_{i=1}^n \mathbf{X}_i g\left(\left\|\frac{\mathbf{X}_i - \mathbf{x}}{h}\right\|^2\right)}{\sum_{i=1}^n g\left(\left\|\frac{\mathbf{X}_i - \mathbf{x}}{h}\right\|^2\right)} - \mathbf{x} \right) \\ &= \hat{f}_{h,G}(\mathbf{x}) \frac{2c_{k,d}}{h^2 c_{g,d}} \mathbf{m}_{h,G}(\mathbf{x}), \end{aligned}$$

with

$$\hat{f}_{h,G}(\mathbf{x}) := \frac{c_{g,d}}{nh^d} \sum_{i=1}^n g\left(\left\|\frac{\mathbf{X}_i - \mathbf{x}}{h}\right\|^2\right) \quad \text{and} \quad \mathbf{m}_{h,G}(\mathbf{x}) := \frac{\sum_{i=1}^n \mathbf{X}_i g\left(\left\|\frac{\mathbf{X}_i - \mathbf{x}}{h}\right\|^2\right)}{\sum_{i=1}^n g\left(\left\|\frac{\mathbf{X}_i - \mathbf{x}}{h}\right\|^2\right)} - \mathbf{x},$$

the KDE with kernel  $G$  and the *mean shift*  $\mathbf{m}_{h,G}$ , respectively. A new candidate  $\mathbf{x}_{\text{new}}$  for the mode ideally satisfy  $D\hat{f}_{h,K}(\mathbf{x}_{\text{new}}) = 0$ , or equivalently  $\mathbf{m}_{h,G}(\mathbf{x}_{\text{new}}) = 0$ , whenever  $\hat{f}_{h,G}(\mathbf{x}_{\text{new}}) > 0$ . We mimic this by setting  $\mathbf{x}_{\text{new}} = \mathbf{x} + \mathbf{m}_{h,G}(\mathbf{x})$ . This leads to Algorithm 1.

If  $K$  has a monotonically decreasing profile  $k$ , the sequence of  $\mathbf{y}$  and  $\hat{f}_{h,K}(\mathbf{y})$  converge and the latter is monotonically increasing. For the Gaussian-kernel we have

$$k(y) = \exp(-y/2) \quad \text{and} \quad K(\mathbf{y}) = (2\pi)^{-d/2} \exp(-\|\mathbf{y}\|^2/2),$$

with profile

$$g(y) = \frac{1}{2} \exp(-y/2) \quad \text{and} \quad G(\mathbf{y}) = K(\mathbf{y}).$$

For given data the number of steps for convergence depends on the chosen kernel. If  $G$  is the uniform kernel the number of steps are finite, otherwise the algorithm should be stopped if the length of the mean shift vector is below a certain threshold; see Comaniciu et al. (2002).

## 2.2 Subspace Constraint Mean Shift Algorithm

The subspace constraint mean shift algorithm (SCMS) is a modification of the mean shift algorithm. It was first proposed by Ozertem and Erdogmus (2011). We move in direction of a projected mean shift vector to



find a ridge point, where we project onto the space spanned by the  $d - s$  eigenvectors, corresponding to the  $d - s$  largest eigenvalues of the estimated negative Hessian of the log-density, called the *local covariance-inverse*. Replacing the Hessian of the density with the Hessian of the log-density does not change the ridge; see Ozertem and Erdogmus (2011).

Using KDE leads to the matrix

$$-\frac{D^2 \hat{f}_{h,K}(\mathbf{x})}{\hat{f}_{h,K}(\mathbf{x})} + \frac{D \hat{f}_{h,K}(\mathbf{x}) D \hat{f}_{h,K}(\mathbf{x})^\top}{\hat{f}_{h,K}(\mathbf{x})^2} = -D^2 \log \hat{f}_{h,K}(\mathbf{x}).$$

We will use the positive Hessian of the log-density, hence we project on the  $d - s$  eigenvectors corresponding to the  $d - s$  largest eigenvalues. The procedure is explained in Algorithm 2.

**Bias.** The SCMS algorithm finds the ridge points of the underlying kernel density estimator, this leads to a ridge estimation of  $K_h * f$  instead of  $f$ . If the kernel fulfills (K0-2), then this is asymptotically

$$\hat{f}_n(\mathbf{x}) = f(\mathbf{x}) + O(h^2) + O_p(n^{-1/2}h^{-d/2}) \quad \text{uniformly in } \mathbf{x} \in \mathbb{R}^d,$$

see also Section ?? . In Genovese et al. (2014) it is shown, that under some regularity conditions on  $f$ , we have

$$\text{Haus}(R(f), R(K_h * f)) = O(h^2),$$

where

$$\text{Haus}(A, B) := \inf\{\delta : A \subset B \oplus \delta \text{ and } B \subset A \oplus \delta\}$$

is the Hausdorff distance with

$$S \oplus \delta := \{\mathbf{s} + \mathbf{z} : \mathbf{s} \in S, \mathbf{z} \in \mathbb{R}^d \text{ with } \|\mathbf{z}\| \leq \delta\} \quad \text{for } S \subset \mathbb{R}^d.$$

Hence, the bias of the density estimation also effects the ridge estimation.

**Uncertainty measure.** The local uncertainty measure defined in Chen et al. (2015a) is given by

$$\rho(\mathbf{x})^2 := \begin{cases} \mathbb{E}(d^2(\mathbf{x}, \hat{R})), & \text{if } \mathbf{x} \in R(K_h * f), \\ 0, & \text{otherwise,} \end{cases}$$

where  $\hat{R}$  is the estimated ridge and  $d(\mathbf{x}, A) := \min\{\|\mathbf{x} - \mathbf{y}\| : \mathbf{y} \in A\}$  for any compact  $A \subset \mathbb{R}^d$ . It can be used for showing the uncertainty of an estimated ridge point, unfortunately, it only takes into account the variance part but not the bias part.

Chen et al. (2015a) also developed an algorithm for estimating  $\rho(\mathbf{x})$  based on bootstrap samples and show consistency thereof; see Chen et al. (2015a, Theorem 5). Moreover, they also show consistency for a bootstrap confidence set for the smoothed ridge  $R(K_h * f)$ .

## 2.3 Log-Concave Ridge Search Algorithm

The log-concave ridge search (LCRS) is based on Definition 1.3. For a starting point  $\mathbf{x}$  we look for the direction with smallest weighted variance, project the weighted data onto the (affine) subspace spanned by those directions and iterate to the mode of the log-concave density estimated from the weighted projected data. We repeat this step until the step-size is below a chosen threshold. The algorithm can be used to find  $(d - 1)$ -dimensional ridges.

---

**Algorithm 3:** Log-Concave Ridge Search

---

**Data:**  $\mathbf{X}_1, \mathbf{X}_2, \dots, \mathbf{X}_n$   
**Input:** Starting point  $\mathbf{x}$ , bandwidth  $h > 0$ ,  $\text{tol} > 0$   
**Result:** Ridge point of  $f$  close to  $\mathbf{x}$   
**begin**  
     $m \leftarrow 2 \text{ tol}$   
    **while**  $|m| > \text{tol}$  **do**  
         $\mathbf{H} \leftarrow \mathbf{S}_n(\mathbf{x}) / s_n(\mathbf{x}) - \mathbf{s}_n(\mathbf{x}) \mathbf{s}_n(\mathbf{x})^\top / s_n(\mathbf{x})^2$   
         $\mathbf{v} \leftarrow \mathbf{V}_\perp(\mathbf{H})$   
         $\mathbf{w}_i \leftarrow s_n(\mathbf{x})^{-1} K_h(\mathbf{X}_i - \mathbf{x})$  for  $1 \leq i \leq n$   
         $\mathbf{z}_i \leftarrow \mathbf{v}^\top (\mathbf{X}_i - \mathbf{x})$  for  $1 \leq i \leq n$   
         $m \leftarrow \text{mode}(\hat{\theta}(\mathbf{z}, \mathbf{w}))$   
         $\mathbf{x} \leftarrow \mathbf{x} + m \mathbf{v}$   
    **return**  $\mathbf{x}$

---

**Finding Direction.** For a point  $\mathbf{x}$  we chose the direction of smallest conditional variance. Therefore, consider the empirical measure

$$\hat{Q}_{\mathbf{x}, n, h} := \sum_{i=1}^n w_i(\mathbf{x}) \delta_{\mathbf{X}_i - \mathbf{x}}, \quad \text{where} \quad w_i(\mathbf{x}) = s_{n, h}(\mathbf{x})^{-1} n^{-1} K_h(\mathbf{X}_i - \mathbf{x})$$

with  $s_{n, h}(\mathbf{x}) := n^{-1} \sum_{i=1}^d K_h(\mathbf{X}_i - \mathbf{x})$ . The empirical conditional variance is then

$$\begin{aligned}
\hat{\Sigma}_{n, h}(\mathbf{x}) &:= \text{Var}(\hat{Q}_{\mathbf{x}, n, h}) \\
&= \sum_{i=1}^n w_i(\mathbf{x}) (\mathbf{X}_i - \mathbf{x}) (\mathbf{X}_i - \mathbf{x})^\top - \left( \sum_{i=1}^n w_i(\mathbf{x}) (\mathbf{X}_i - \mathbf{x}) \right) \left( \sum_{i=1}^n w_i(\mathbf{x}) (\mathbf{X}_i - \mathbf{x}) \right)^\top \\
&= h^2 \left( \frac{\mathbf{S}_{n, h}(\mathbf{x})}{s_{n, h}(\mathbf{x})} - \frac{\mathbf{s}_{n, h}(\mathbf{x}) \mathbf{s}_{n, h}(\mathbf{x})^\top}{s_{n, h}(\mathbf{x})^2} \right),
\end{aligned}$$

with

$$\begin{aligned}
\mathbf{s}_{n, h}(\mathbf{x}) &:= \frac{1}{n} \sum_{i=1}^n K_h(\mathbf{X}_i - \mathbf{x}) h^{-1} (\mathbf{X}_i - \mathbf{x}), \\
\mathbf{S}_{n, h}(\mathbf{x}) &:= \frac{1}{n} \sum_{i=1}^n K_h(\mathbf{X}_i - \mathbf{x}) h^{-2} (\mathbf{X}_i - \mathbf{x}) (\mathbf{X}_i - \mathbf{x})^\top.
\end{aligned}$$

We have

$$\hat{\Sigma}_{n, h}(\mathbf{x}) = h^2 \mathbf{I}_d + h^4 D^2 \ell(\mathbf{x}) + o(h^4) + O_p(n^{-1/2} h^{-d/2-2})$$

and by Lemma 1.5 we get

$$\hat{\Sigma}_{n, h}(\mathbf{x}) - \Sigma_h(\mathbf{x}) = o(h^4) + O_p(n^{-1/2} h^{-d/2-2}) \quad \text{as} \quad h \rightarrow 0.$$

Hence we have a consistent estimator of the direction of smallest conditional variance, whenever  $nh^{d+4} \rightarrow \infty$ . This direction is then the eigenvector of  $\hat{\Sigma}_{n, h}(\mathbf{x})$  corresponding to the smallest eigenvalue, this is  $\mathbf{v} := \mathbf{V}_\perp(\hat{\Sigma}_{n, h}(\mathbf{x}))$ . The following theorem shows, that a small perturbation of  $\mathbf{x}$  only leads to a small perturbation of  $\hat{\Sigma}_{n, h}(\mathbf{x})$ , whence only to a small perturbation of  $\mathbf{v}$ .

**Theorem 2.1** (Lipschitz Continuity). *Let  $f \in \mathcal{C}^2(\mathbb{R}^d)$  and suppose (K0-2) and (K5) hold. For a sample  $\mathcal{X} = \{\mathbf{X}_1, \dots, \mathbf{X}_n\}$  and fixed  $h$ , the local sample variance is Lipschitz continuous on the convex hull of the sample, i.e.*

$$\|\widehat{\Sigma}_{n,h}(\mathbf{x}) - \widehat{\Sigma}_{n,h}(\mathbf{y})\|_F \leq L\|\mathbf{x} - \mathbf{y}\| \quad \text{for } \mathbf{x}, \mathbf{y} \in \text{conv}(\mathbf{X}_1, \dots, \mathbf{X}_n),$$

*whenever there exists  $0 < \tau \leq s_n(\mathbf{x})$  for all  $\mathbf{x} \in \text{conv}(\mathbf{X}_1, \dots, \mathbf{X}_2)$ , with some  $L > 0$  depending on the sample, the kernel  $K$  and bandwidth  $h$ .*

**Finding mode of projection.** For a point  $\mathbf{x}$  and the direction  $\mathbf{v}$  we define

$$z_i = \mathbf{v}^\top (\mathbf{X}_i - \mathbf{x}) \quad \text{with weights} \quad w_i = s_n(\mathbf{x})^{-1} K_h(\mathbf{X}_i - \mathbf{x}) \quad \text{for } 1 \leq i \leq n.$$

These leads the empirical measure

$$\widehat{P}_{\mathbf{x},n,h} := \sum_{i=1}^n w_i \delta_{z_i}. \quad (1)$$

We use the maximum likelihood estimation for log-concave distributions proposed in Dümbgen and Rufibach (2009). The algorithm is explained in Dümbgen and Rufibach (2011) and refined in Dümbgen et al. (2018). The estimated log-density  $\widehat{\theta}(\mathbf{z}, \mathbf{w})$  with  $\mathbf{z} = (z_1, \dots, z_n)$  and  $\mathbf{w} = (w_1, \dots, w_n)$  is piecewise linear with change of slope at data points, convex and unique. Hence, the algorithm will return a unique mode  $m$  almost surely. We update the considered point to  $\mathbf{x} + m\mathbf{v}$ .

**Interpretation of direction.** A log-transformation of the density does not change the ridge set. However, in case of a Gaussian distribution with covariance matrix  $\Sigma$ , the Hessian of the log-density is independent of location and equal to

$$D^2 \log f(\mathbf{x}) = -2^{-1} \Sigma^{-1}.$$

The  $d - s$  eigenvectors associated to the  $d - s$  largest eigenvalues coincide with the  $d - s$  last linear principle components of the distribution. Hence, using the log-transformation gives a beneficial interpretation of the considered subspace.

The conditional covariance matrix  $\text{Var}(\mathbf{X} | \mathbf{X} + \mathbf{Z}_h = \mathbf{x})$  leads the same interpretation. For a Gaussian distribution  $\mathbf{X}$ , the conditional distribution of  $\mathbf{X}$ , given  $\mathbf{X} + \mathbf{Z}_h = \mathbf{x}$  with  $\mathbf{Z}_h \sim \mathcal{N}(\mathbf{0}, h^2 \mathbf{I}_d)$  for  $h > 0$  is Gaussian as well and the considered subspace coincides with the  $d - s$  last linear principle components. Another interpretation of the conditional covariance matrix is as the  $(d - s)$ -dimensional subspace with conditional least variance. Hence, the ridge is in direction of largest variance.

**Bandwidth selection.** One crucial part of the algorithms is selecting the bandwidth. Whereas in the calculation of the mode via log-concave density estimation, the result does not change drastically for different bandwidths, it can have an effect on the conditional variance and the resulting direction of smallest conditional variance. Therefore, we will focus on a suitable bandwidth for the latter.

In Chen et al. (2015b) they recommend choosing  $h$  via

$$h = A_0(d+2)^{-1/(d+4)} n^{-1/(d+4)} \sigma_{\min}, \quad (2)$$

where  $A_0$  is some constant,  $d$  is the dimension and  $\sigma_{\min}$  is the minimal value for the standard deviation along each coordinate. For  $A_0 = 1$ , one obtains Silverman's rule; see Silverman (1986).

Another choice is using a functional of the length of the euclidean minimal spanning tree (EMST) as bandwidth. For a sample  $\mathbf{X}_1, \dots, \mathbf{X}_n$  consider the fully connected, undirected graph  $G = (V, E)$  with

vertices  $V = \{\mathbf{X}_1, \dots, \mathbf{X}_n\}$  and edges  $E = \{(\mathbf{X}_i, \mathbf{X}_j) : 1 \leq i < j \leq n\}$ . The EMST is the graph  $E_n := E_n(\mathbf{X}_1, \dots, \mathbf{X}_n) \subset G$  that connects all vertices in  $V$  such that the total edge length is minimized. Let  $L_n$  be the length of  $E_n(\mathbf{X}_1, \dots, \mathbf{X}_n)$ , then we chose the bandwidth as

$$h_n = \left(\frac{L_n}{n}\right)^{1/(d+4)}. \quad (3)$$

In Sreevani and Murthy (2016) they use

$$T_n = \left(\frac{L_n}{n}\right)^{1/d}$$

as a bandwidth for the kernel density estimator and show that  $L_n \rightarrow \infty$ ,  $h_n \rightarrow 0$  and  $nT_n^d \xrightarrow{p} \infty$  as  $n \rightarrow \infty$  under some mild conditions on the kernel and the density function, the most restrictive being compact support of the density function. From those two results we get immediately, that  $nh_n^{d+4} \xrightarrow{p} \infty$  as  $n \rightarrow \infty$ , the desired rate for estimating  $D^2 \log f(\mathbf{x})$  consistently in case of  $f \in \mathcal{C}^2(\mathbb{R}^d)$ . Because it is

$$\begin{aligned} h^{-4} \widehat{\Sigma}_{n,h}(\mathbf{x}) - D^2 \log f(\mathbf{x}) &= h^{-4} (\widehat{\Sigma}_{n,h}(\mathbf{x}) - \Sigma_h(\mathbf{x})) + h^{-4} \Sigma_h(\mathbf{x}) - D^2 \log f(\mathbf{x}) \\ &= O_p(n^{-1/2} h^{-d/2-2}) + o(1) \\ &= o_p(1) \quad \text{if } nh^{d+4} \rightarrow \infty. \end{aligned}$$

**Confidence region of the ridge.** For each point  $\mathbf{x}$  on the estimated ridge one can calculate a confidence interval along the direction  $\mathbf{v} := \mathbf{V}_\perp(\widehat{\Sigma}_{n,h}(\mathbf{x}))$  by using the likelihood ratio test suggested in Doss and Wellner (2019).

Let  $\mathcal{P}$  be the family of all log-concave densities on  $\mathbb{R}$ . Suppose  $g = e^\varphi \in \mathcal{P}$ , where  $\varphi$  has second derivative  $\varphi''$  at the mode  $m(g)$  and satisfies  $\varphi''(m) < 0$ . Consider the following testing problem:  $H_0 : m(g) = m$  versus  $H_1 : m(g) \neq m$ , where  $m \in \mathbb{R}$  is fixed. One can then calculate the unconstrained maximum likelihood estimator (MLE)  $\widehat{g}_n$  and the mode-constrained MLE  $\widehat{g}_n^o$  with  $m(\widehat{g}_n^o) = m$ . Those two functions lead to the log-likelihood statistic, given by

$$2 \log \lambda_n = 2 \log \lambda_n(m) = 2n \mathbb{P}_n(\log \widehat{g}_n - \log \widehat{g}_n^o) = 2n \mathbb{P}_n(\widehat{\varphi}_n - \widehat{\varphi}_n^o),$$

where  $\widehat{\varphi} = \log \widehat{g}_n$ ,  $\widehat{\varphi}^o = \log \widehat{g}_n^o$ ,  $\mathbb{P}_n = \sum_{i=1}^n w_i \delta_{X_i}$ , and  $\mathbb{P}_n(q) = \int q d\mathbb{P}_n$ .

**Theorem 2.2** (Theorem 1.1 in Doss and Wellner (2019)). *If  $X_1, X_2, \dots, X_n$  are i.i.d.  $g = e^\varphi$  with mode  $m$ , where  $\varphi$  is concave, twice continuously differentiable at  $m$ , and  $\varphi''(m) < 0$ , then*

$$2 \log \lambda_n \xrightarrow{d} \mathbb{D},$$

where  $\mathbb{D}$  is a universal limiting distribution.

Let  $c_\alpha$  be such that  $\mathbb{P}(\mathbb{D} > \alpha) = \alpha$ , where the distribution of  $\mathbb{D}$  can be approximated by Monte Carlo methods. We can reject  $H_0$  at level  $\alpha$ , whenever  $2 \log \lambda_n > c_\alpha$ . A asymptotic  $\alpha$ -confidence interval for the mode is then given by

$$I_\alpha(\mathbb{P}_n) = \{m \in \mathbb{R} : 2 \log \lambda_n(m) \leq c_\alpha\}.$$

We apply this procedure for the measure  $\widehat{P}_{\mathbf{x},n,h}$  for  $\mathbf{x}$  on the estimated ridge and get the one-dimensional confidence region

$$\{\mathbf{x} + t\mathbf{v} : t \in I_\alpha(\widehat{P}_{\mathbf{x},n,h})\}.$$

Of course, this doesn't lead by any means to a confidence region. However, it can be seen as a measure of uncertainty.

**Threshold intervals for the ridge.** An issue of the LCRS is whenever the projected weighted density function is rather flat close to the mode, a small change of the initial point may lead to a different estimated mode in the next step of the algorithm, and whence to ridge points far away from each other. In Figure 1 we see two different, but very close, starting points leading to different modes in the first step. After 1 and 8 steps, respectively, the algorithm stops for both starting points at different modes. However, looking at the threshold interval, they are very close to each other; see Figure 2 and 3.

Instead of only reporting the estimated ridge point, we use the estimated log-concave density  $\hat{\theta}$  to find the interval

$$I(\hat{\theta}) := \{x \in \mathbb{R} : \hat{\theta}(x) \geq m + \log(\tau)\} = \{x \in \mathbb{R} : e^{\hat{\theta}(x)} \geq \tau e^{\hat{\theta}(m)}\}.$$

Thus, we get a uncertainty measure for the ridge. The threshold interval is computationally much less expensive then the confidence intervals.

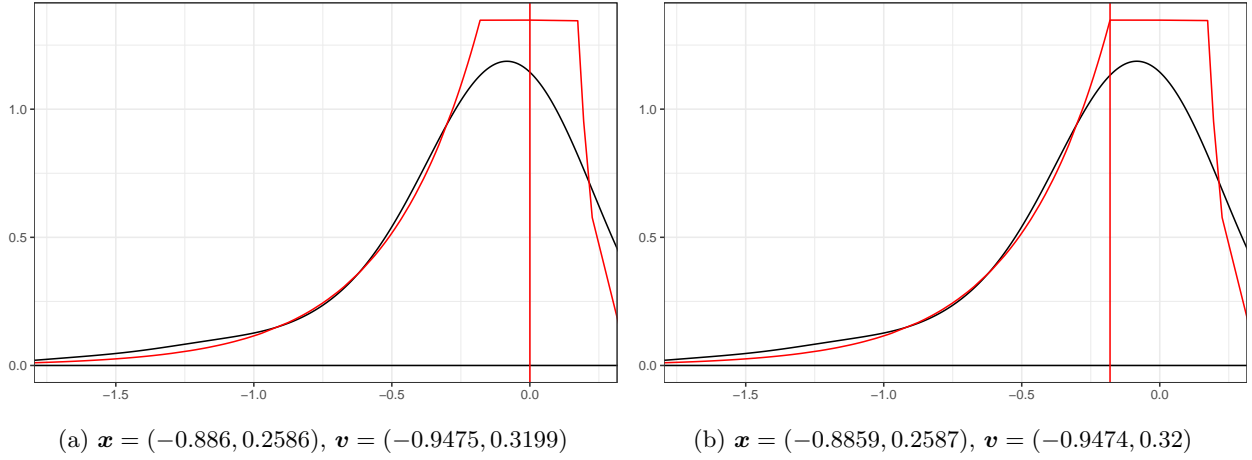


Figure 1: Shows the estimated projected weighted log-concave density estimator (red) and the kernel density estimator (black), for two slightly different starting points. The mode is indicated by the vertical line.

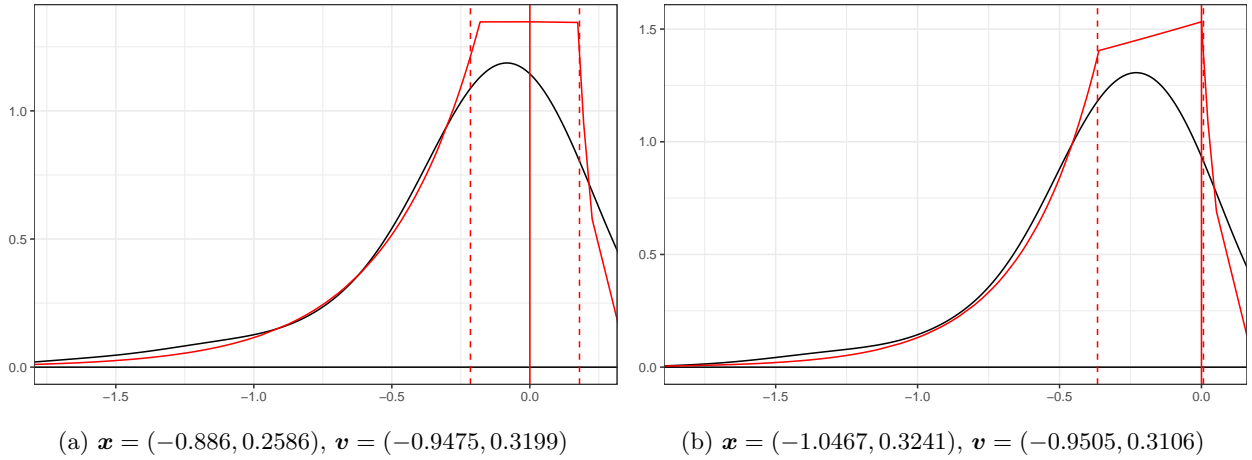


Figure 2: Shows the estimated weighted projected log-concave density estimator (red) and the kernel density estimator (black) after the last step of the algorithm. The red dashed line corresponds to the threshold for  $\alpha = 0.9$ .

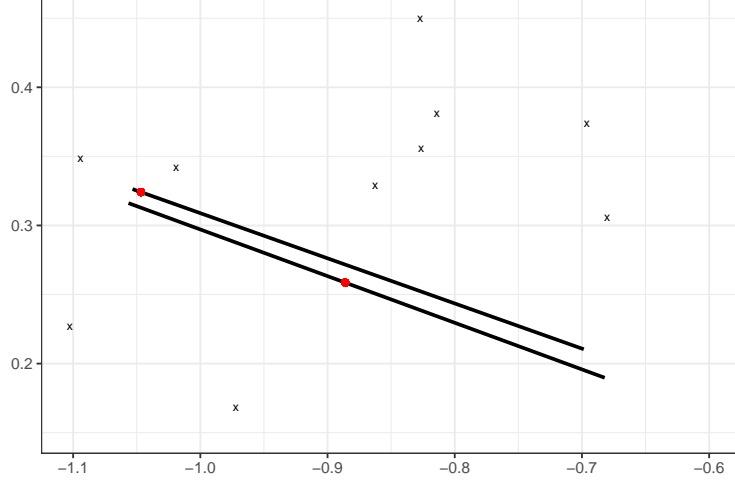


Figure 3: Shows the estimated ridge points (red) and the threshold interval (black) for two slightly different starting points.

**Smoothed ridge.** Another possibility, to avoid the discontinuous behavior of the estimated ridge line, is by replacing the estimated log-density  $\hat{\theta}$  by a smoothed version. Dümbgen and Rufibach (2011) propose

$$\hat{g}^*(y) = \int_{-\infty}^{\infty} \hat{g}(t) \phi_{\gamma}(y - t) dt,$$

where  $\hat{g}(t) = e^{\hat{\theta}(t)}$  and  $\phi_{\gamma}(t) := (2\pi\gamma^2)^{-1/2} \exp(-t^2/(2\gamma^2))$ . This is the convolution of the estimated log-concave density with a Gaussian distribution, where  $\gamma$  is chosen, such that the variance of the new estimator coincides with the variance of the empirical distribution. The mode of  $\hat{g}^*$  can be found by Newton's method. Replacing the mode of  $\hat{\theta}$  by the mode of  $\hat{g}^*$  in Algorithm 3 leads to typically smoother ridge lines. We will refer to it as smoothed LCRS (sLCRS).

### 3 Data Examples

The algorithms have been implemented in the statistical language R R Core Team (2019) and calculations were performed on UBELIX (<http://www.id.unibe.ch/hpc>), the HPC cluster at the University of Bern.

#### 3.1 Circle Data

Suppose we have a sample  $\mathbf{X}_1, \mathbf{X}_2, \dots, \mathbf{X}_n \in \mathbb{R}^2$  with distribution  $\mathcal{P} := \mathcal{L}(\mathbf{X})$ , where

$$\mathbf{X} := r \begin{pmatrix} \cos(2\pi U) \\ \sin(2\pi U) \end{pmatrix} + \sigma \mathbf{Z},$$

with  $r, \sigma \in \mathbb{R}_{>0}$  and independent random variables  $U \sim \mathcal{U}([0, 1])$  and  $\mathbf{Z} \sim \mathcal{N}(0, \mathbf{I}_2)$ . The density function  $f$  of  $\mathcal{P}$  is

$$f(\mathbf{x}) = (2\pi\sigma^2)^{-1} I_0(r/\sigma^2 \|\mathbf{x}\|) \exp\left(-\frac{r^2 + \|\mathbf{x}\|^2}{2\sigma^2}\right),$$

where

$$I_0(t) := \sum_{m=0}^{\infty} \frac{(t^2/4)^m}{(m!)^2}$$

is the modified Bessel function of the first kind with parameter 0. One can show that the ridge of  $f$  is the origin if  $r/\sigma \leq \sqrt{2}$  and a circle with radius in  $(0, r)$  and centre at the origin if  $r/\sigma > \sqrt{2}$ . The exact value can be numerically calculated with bisection; see Section A.1 for details. In our simulation study we use  $n = 200$  data points with  $r = 1$  and  $\sigma = 0.1$ , the ridge is then the circle with center  $\mathbf{0}$  and radius 0.995. We estimate the ridge with the SCMS, LCRS and sLCRS algorithm based on the Gaussian kernel  $K_h$  for different bandwidths; see Figure 4.

**Results.** The ridge estimated by SCMS is biased towards the center and the larger the bandwidth  $h$ , the larger the biases. Indeed, let  $\mathbf{Z}_h$  have density function  $K_h$ , then we estimate the Ridge of the random variable  $\mathbf{X} + \mathbf{Z}_h$  instead of  $\mathbf{X}$ , which has the same distribution as circle data with standard deviation  $\sqrt{\sigma^2 + h^2}$  instead of  $\sigma$ .

The ridge estimated by LCRS is not sensitive to the choice of the bandwidth. However, the estimated ridge is discontinuous and we should use confidence or threshold intervals to show this uncertainty; see Figure 5. There we see, that e.g. on the top left, the estimator is very uncertain. A close look at the data reveals indeed, that the data point in this area are spread away from the true ridge, whence the ridge could lay in a wide region. On the top right, the data points are nicely spread around the true ridge and the LCRS catches that well.

For the sLCRS we still get a discontinuous ridge for  $h = 0.2$ . However, for larger bandwidths it is smooth and the bias caused by the smoothing is less serious then for the SCMS.

### 3.2 Galaxy filaments

We apply both algorithms to data from Data Release 16 (Ahumada et al. (2019)) of the Sloan Digital Sky Survey (SDSS); see York et al. (2000) and Eisenstein et al. (2011).

The Baryon Oscillation Spectroscopic Survey (BOSS) is part of the SDSS and obtains the redshift  $z$  from 1.5 million luminous galaxies on 10 000 square degrees of sky in celestial coordinates. The longitude is called right ascension (RA) and the latitude is called declination (Dec). Both are measured in degree.

Th galaxies in our universe are not distributed uniformly, they follow a web structure with clusters, sheets and empty voids. The filaments are one-dimensional structures connecting clusters and build the boundaries of the voids. The knowledge about filaments at the range of different redshifts is interesting for cosmologists to study the evolution of the universe. For more detailed information we refer to Chen et al. (2015b) and the reference therein.

Chen et al. (2015b) used Data Release 12 to estimate galaxy filaments at different redshifts with the SCMS algorithm. We use the same slices of data, namely at

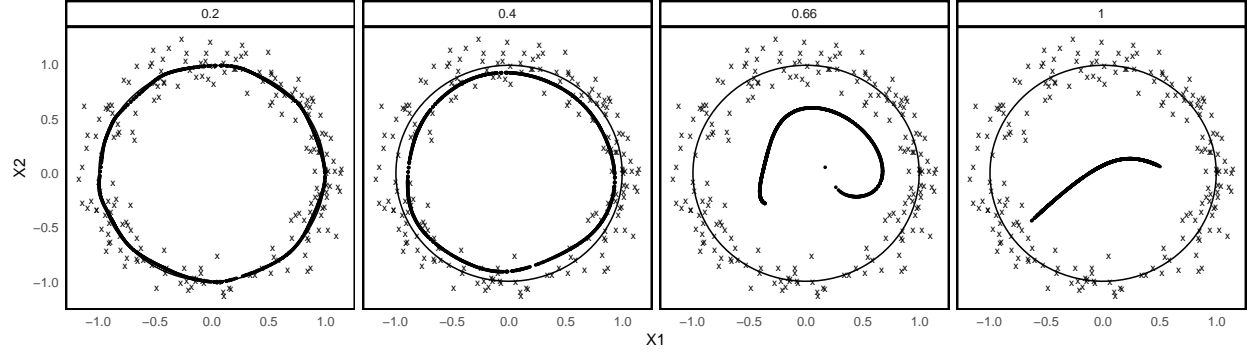
$$135^\circ \leq \text{RA} \leq 175^\circ \quad 5^\circ \leq \text{Dec} \leq 45^\circ \quad 0.245 \leq z \leq 0.240$$

with low redshift and at

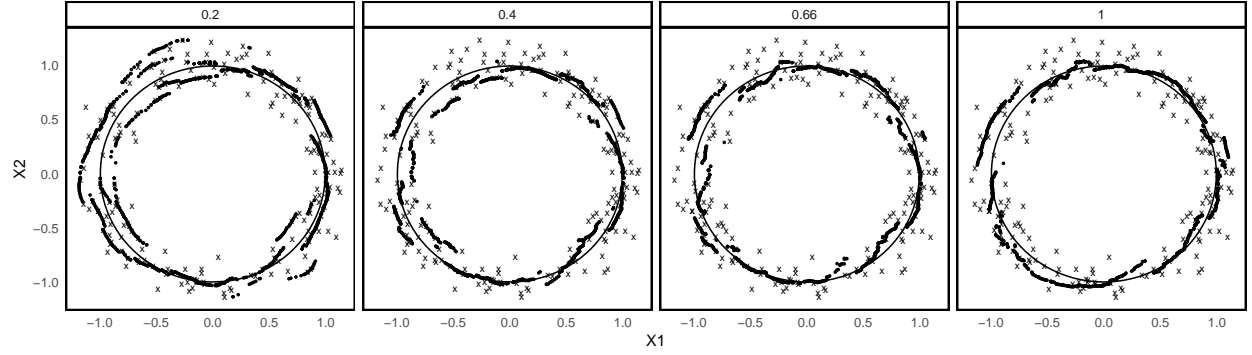
$$135^\circ \leq \text{RA} \leq 175^\circ \quad 5^\circ \leq \text{Dec} \leq 45^\circ \quad 0.530 \leq z \leq 0.535$$

with high redshift. We apply both algorithms to the data for low and high redshift and compare them to each other. The used slice for the algorithms are from  $130^\circ \leq \text{RA} \leq 180^\circ$  and  $0^\circ \leq \text{Dec} \leq 50^\circ$  to avoid

(a) SCMS



(b) LCRS



(c) sLCRS

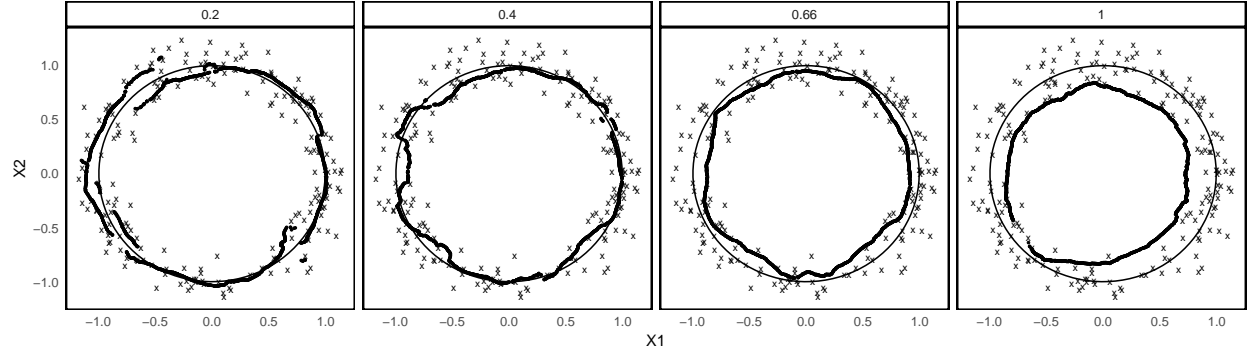


Figure 4: Shows the estimated ridge points for different bandwidths for both algorithms and the true ridge as a solid circle.



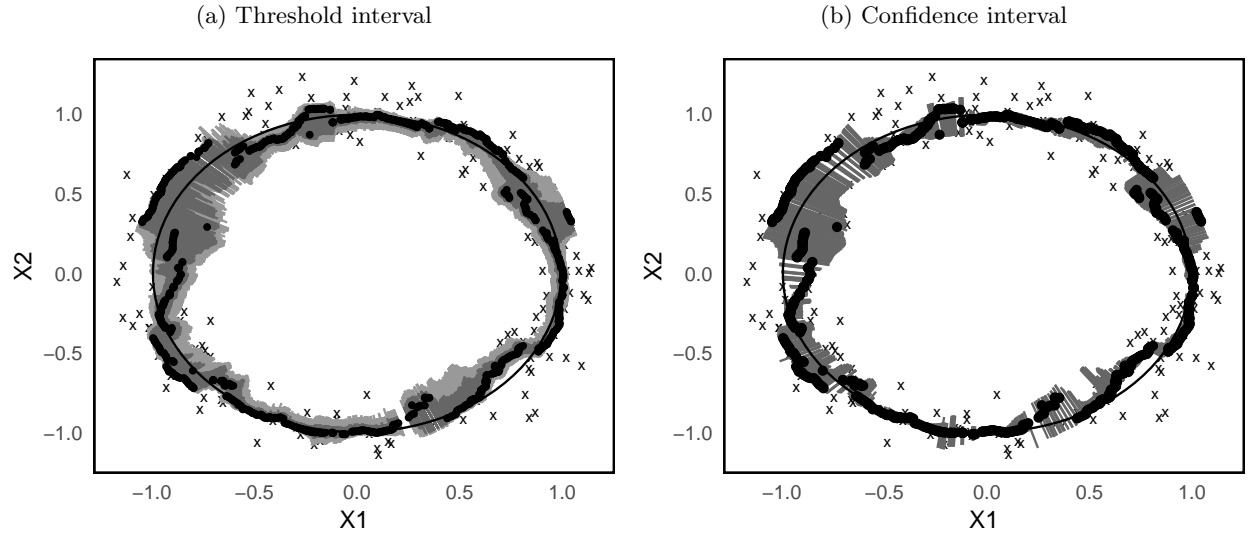


Figure 5: Shows the estimated ridge points and true ridge (black). Left: Threshold interval for  $\alpha \in \{0.8, 0.9\}$ . Right: 90%-Confidence interval for the ridge point in direction of smallest variance.

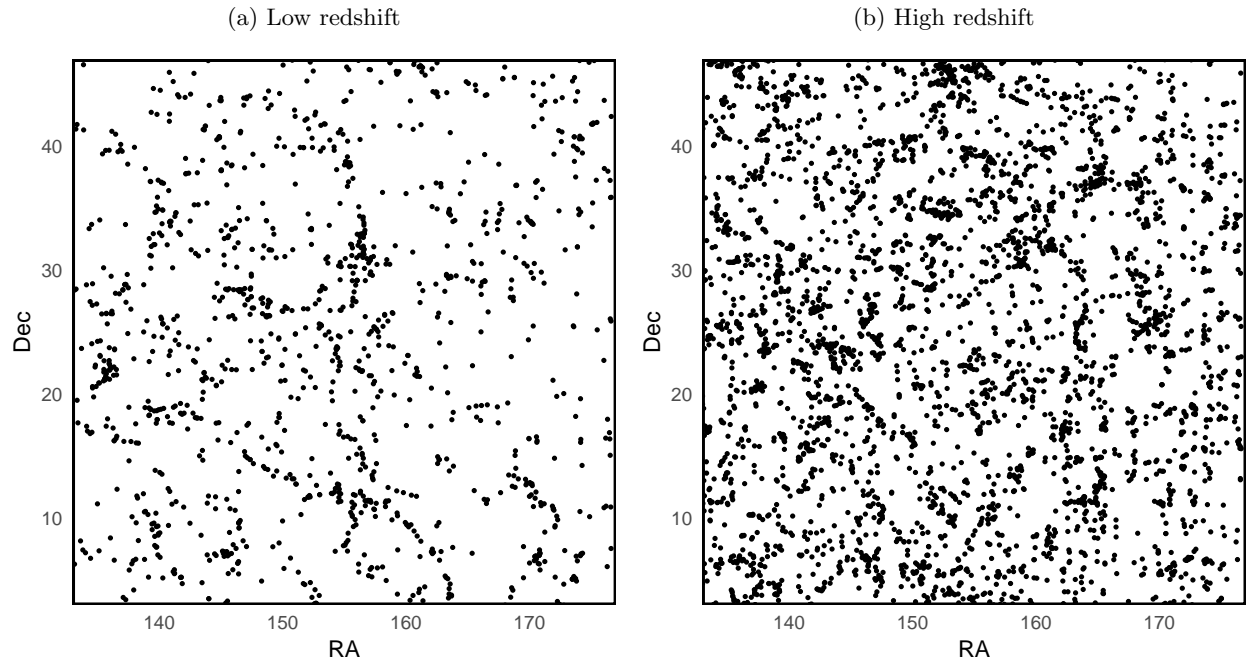


Figure 6: Galaxy structure from the Baryon Oscillation Spectroscopic Survey for a slice of sky at two different redshifts.

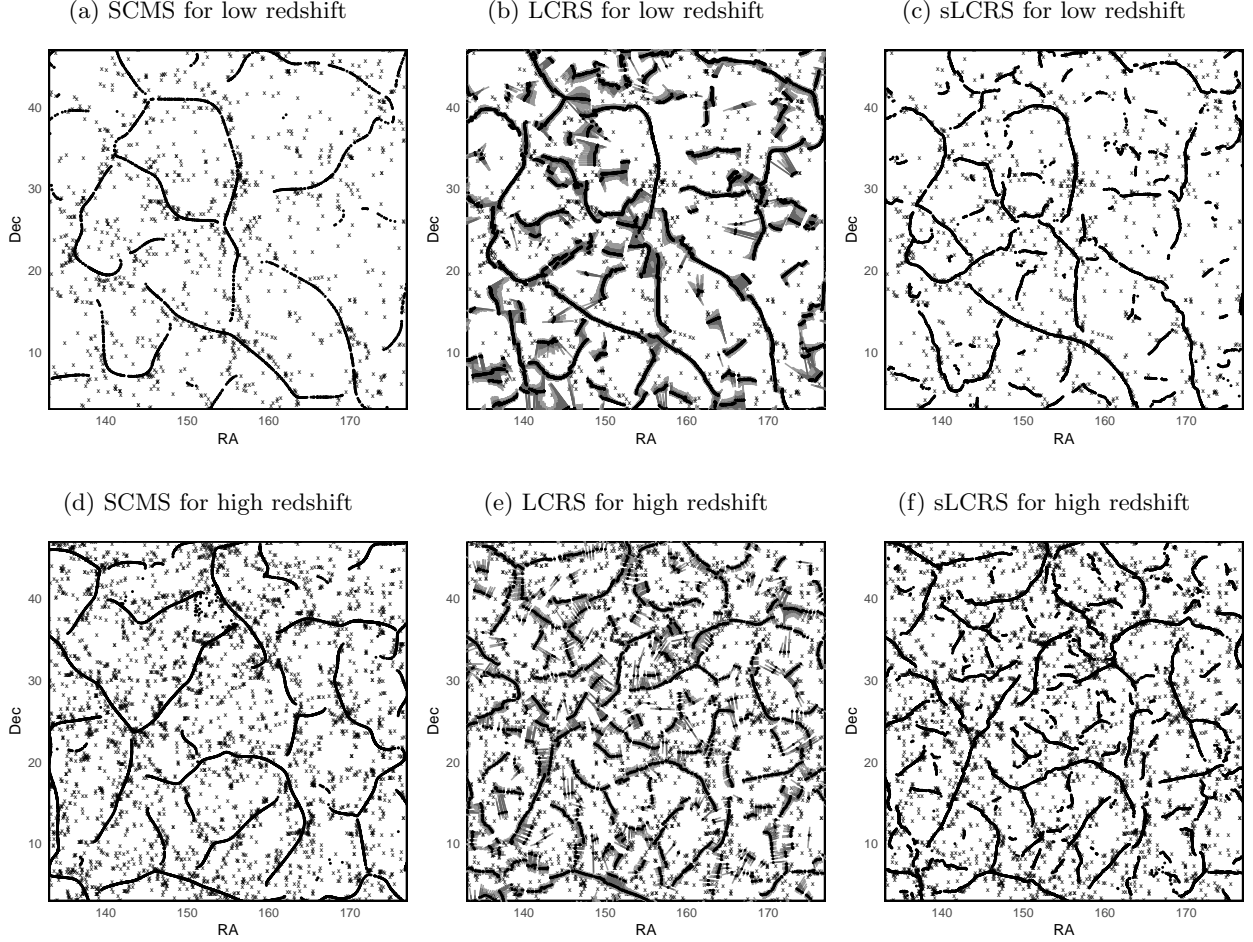


Figure 7: Shows the estimated ridge points (black) for low and high redshift. Threshold interval (grey) with  $\alpha \in \{0.8, 0.9\}$  are drawn for the LCRS. The bandwidth is  $h = 2.03$ .

boundary effects in the estimation. We refrain from analysing the data in 3 dimensions, where redshift could be used as the third one, for different reasons. The obvious one being, that with the LCRS algorithm one can only estimate 1-dimensional ridges in 2 dimensions, but not in 3. Another reason being, that the density of galaxies changes for different redshift, whence, estimating everything with the same bandwidth may be problematic.

We focus on the bandwidth given in (2) with  $A_0 = 0.4$ . This particular choice of  $A_0$  was made in Chen et al. (2015b) by trying different ones on taking the most suitable one, leading to  $h = 2.5$  in the low redshift and  $h = 2.03$  in the high redshift data.

For the high redshift data, we show the results for different bandwidths for the SCMS and LCRS algorithm; see Figure 8 and 9. The optimal bandwidth calculated based on the euclidean minimal spanning tree is  $h = 0.84$ . Additionally, we considered  $h = 1.5$  and  $h = 2.5$ .

As starting points we choose a grid of points with vertical and horizontal distance 0.5 and remove all point further then 0.5 away from any data point. For the low redshift we get 2842 points and for the high redshift data 5777 points. For sLCRS we used a finer grid, where the points lay 0.25 apart, leading to 23080 grid

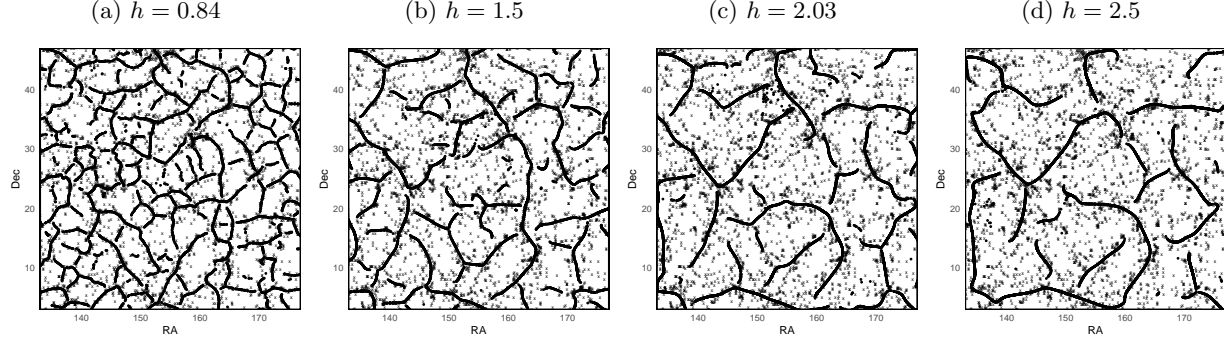


Figure 8: Shows the estimated ridge points for the SCMS with different bandwidths  $h$ .

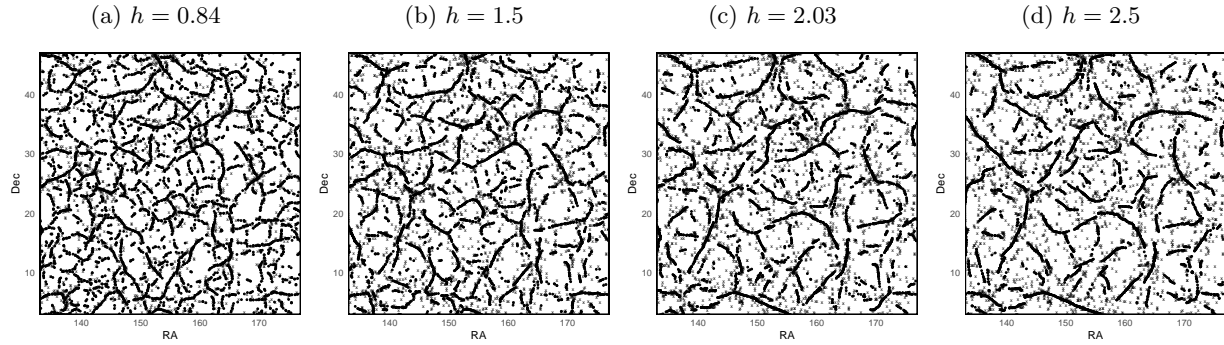


Figure 9: Shows the estimated ridge points for the LCRS with different bandwidths  $h$ .

points. Chen et al. (2015b) chose the data points as starting points and removed those, where the estimated density was below a certain threshold (low redshift:  $1.02 \cdot 10^{-3}$ , high redshift:  $7.52 \cdot 10^{-4}$ ).

**Results.** Looking at the results for the lower redshift data in Figure 7 (a–c), we see that the ridge lines found by the SCMS are also covered by the LCRS and sLCRS. In areas where there is a clear ridge line observable by just looking at the data (i.e. from (145, 20) to (163, 5)), the LCRS and sLCRS algorithms follow it smoothly and go directly through the data. The SCMS is also smooth, but the ridge is closer towards the center of the curvature, and lays above the most data points for smaller Dec and below for larger Dec. Hence one observes the same phenomena as for the simulated circle data in Figure 4a. In areas where there isn't a clear ridge line visible from eye (i.e. around (145, 22)), the LCRS may be fragmented, looking at the threshold intervals reveal, that we have a flat projected weighted density along the smallest variance (compare Figure 4b), whence the ridge may lay somewhere on this flat part, represented by the threshold interval. The sLCRS finds a smooth ridge in this area through the data points. The ridge estimated by the SCMS is interrupted and again biased towards the center of the curvature.

The results for the high redshift data in Figure 7 (d–f) show the same effects as for the low redshift data.

In Figure 8–10 we look at the estimated ridges for different bandwidths for the high redshift data. For all algorithms the number of ridge lines get lower and the ridge lines getting longer as the bandwidth increases. This effect is most distinctive for the SCMS algorithm. For the LCRS algorithm, even for larger bandwidth there are still some short ridge line visible. However, in case of the SCMS algorithm we notice, that the

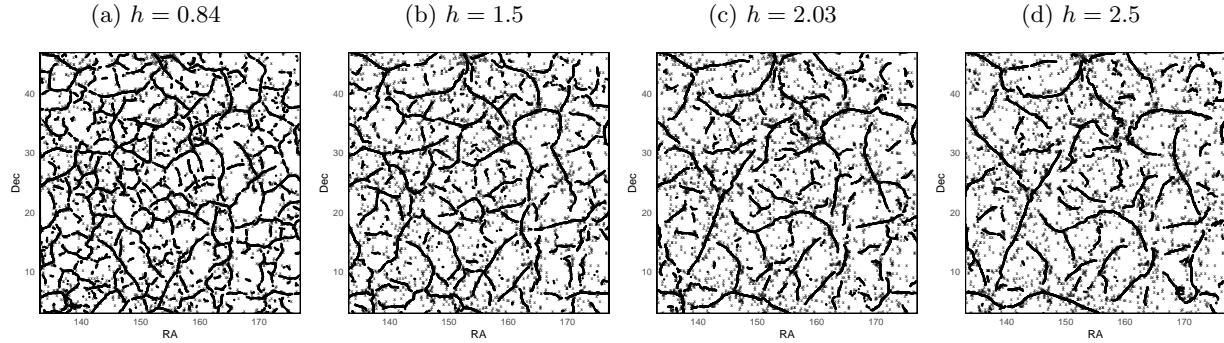


Figure 10: Shows the estimated ridge points for the sLCRS with different bandwidths  $h$ .

ridges move around for different bandwidths, e.g. the ridge from (150, 20) to (160, 5) goes from a zigzag-shape to a round c-shape. In case of the LCRS and sLCRS algorithm the estimated ridge does not move around for different bandwidths, it just gets less connected for lower bandwidths.

### 3.3 Discussion

In the simulated and the real data example we see that the performance of the SCMS algorithm strongly depends on the bandwidth choice. This is evident for the circle data with high bandwidths (Figure 4a), but also for the galaxy data. For the LCRS algorithm this effect does not occur and for the sLCRS algorithm it is small. Hence, LCRS and sLCRS is much more robust regarding bandwidth selection then the SCMS.

Therefore, whenever one is not only interested in estimating a smooth (but possibly biased) ridge, we recommend using LCRS algorithm with threshold intervals in case one wants a uncertainty measure or sLCRS if one wants smooth ridges that are not biased.

**Acknowledgements.** This work was supported by Swiss National Science Foundation. I'm grateful to Johanna F. Ziegel and Lutz Dümbgen for their support and valuable inputs.

## References

- R. Ahumada et al. The sixteenth data release of the sloan digital sky surveys: First release from the APOGEE-2 southern survey and full release of eBOSS spectra. *The Astrophysical Journal Supplement Series*, 249(1), 2019.
- R. Bhatia. *Matrix analysis*, volume 169 of *Graduate Texts in Mathematics*. Springer-Verlag, New York, 1997.
- Y.-C. Chen, C. R. Genovese, and L. Wasserman. Asymptotic theory for density ridges. *The Annals of Statistics*, 43(5):1896–1928, 10 2015a.
- Y.-C. Chen, S. Ho, P. E. Freeman, C. R. Genovese, and L. Wasserman. Cosmic web reconstruction through density ridges: method and algorithm. *Monthly Notices of the Royal Astronomical Society*, 454(1):1140–1156, 09 2015b.

- Y. Cheng. Mean shift, mode seeking, and clustering. *IEEE Transactions on Pattern Analysis and Machine Intelligence*, 17(8):790–799, 1995.
- D. Comaniciu, P. Meer, and S. Member. Mean shift: A robust approach toward feature space analysis. *IEEE Transactions on Pattern Analysis and Machine Intelligence*, 24:603–619, 2002.
- P. Delicado. Another look at principal curves and surfaces. *Journal of Multivariate Analysis*, 77(1):84–116, 2001.
- P. Delicado and M. Huerta. Principal curves of oriented points: theoretical and computational improvements. *Computational Statistics*, 18(2):293–315, 2003. Euroworkshop on Statistical Modelling (Bernried, 2001).
- C. R. Doss and J. A. Wellner. Inference for the mode of a log-concave density. *The Annals of Statistics*, 47(5):2950–2976, 2019.
- L. Dümbgen and K. Rufibach. Maximum likelihood estimation of a log-concave density and its distribution function: basic properties and uniform consistency. *Bernoulli*, 15(1):40–68, 2009.
- L. Dümbgen and K. Rufibach. logcondens: Computations related to univariate log-concave density estimation. *Journal of Statistical Software*, 39(i06), 2011.
- L. Dümbgen, A. Moesching, and C. Strähl. Active set algorithms for estimating shape-constrained density ratios, 2018.
- D. Eberly. *Ridges in Image and Data Analysis*. Computational Imaging and Vision. Springer Netherlands, 1996.
- D. J. Eisenstein et al. SDSS-III: Massive spectroscopic surveys of the distant universe, the milky way, and extra-solar planetary systems. *The Astronomical Journal*, 142(3):72, 2011.
- C. R. Genovese, M. Perone-Pacifico, I. Verdinelli, and L. Wasserman. Nonparametric ridge estimation. *The Annals of Statistics*, 42(4):1511–1545, 2014.
- T. Hastie and W. Stuetzle. Principal curves. *Journal of the American Statistical Association*, 84(406):502–516, 1989.
- B. Kégl, A. Krzyzak, T. Linder, and K. Zeger. Learning and design of principal curves. *IEEE Transactions on Pattern Analysis and Machine Intelligence*, 22(3):281–297, 2000.
- U. Ozertem and D. Erdogmus. Locally defined principal curves and surfaces. *Journal of Machine Learning Research*, 12:1249–1286, 2011.
- R Core Team. *R: A Language and Environment for Statistical Computing*. R Foundation for Statistical Computing, Vienna, Austria, 2019.
- B. W. Silverman. *Density estimation for statistics and data analysis*. Monographs on Statistics and Applied Probability. Chapman & Hall, London, 1986.
- H. C. Simpson and S. J. Spector. Some monotonicity results for ratios of modified Bessel functions. *Quarterly of Applied Mathematics*, 42(1):95–98, 1984.
- Sreevani and C. Murthy. On bandwidth selection using minimal spanning tree for kernel density estimation. *Computational Statistics and Data Analysis*, 102:67–84, 2016.
- C. Strähl, J. F. Ziegel, and L. Dümbgen. Local estimation of a multivariate density and its derivatives. Preprint. Available at <https://arxiv.org/abs/1812.09322>, 2020.
- D. G. York et al. The sloan digital sky survey: Technical summary. *The Astronomical Journal*, 120(3):1579–1587, 2000.

## A Auxiliary Results

### A.1 Ridge of circle data

Suppose we have a sample  $\mathbf{X}_1, \mathbf{X}_2, \dots, \mathbf{X}_n \in \mathbb{R}^2$  with distribution  $\mathcal{P} := \mathcal{L}(\mathbf{X})$ , where

$$\mathbf{X} := r \begin{pmatrix} \cos(2\pi U) \\ \sin(2\pi U) \end{pmatrix} + \sigma \mathbf{Z},$$

with  $r, \sigma \in \mathbb{R}_{>0}$  and independent random variables  $U \sim \mathcal{U}([0, 1])$  and  $\mathbf{Z} \sim \mathcal{N}(0, \mathbf{I}_2)$ .

Let  $f$  be the probability density function of the distribution  $\mathcal{P}$ , by the law of total probability we have

$$\begin{aligned} f(\mathbf{x}) &= \int_0^1 f_{\mathbf{Z}}(\mathbf{x} | U = u) du \\ &= (2\pi\sigma^2)^{-1} \int_0^1 \exp\left(-\frac{r^2 - 2r(x_1 \cos(2\pi u) + x_2 \sin(2\pi u)) + \|\mathbf{x}\|^2}{2\sigma^2}\right) du \\ &= (4\pi^2\sigma^2)^{-1} \exp\left(-\frac{r^2 + \|\mathbf{x}\|^2}{2\sigma^2}\right) \int_0^{2\pi} \exp\left(\frac{r}{\sigma^2}(x_1 \cos(u) + x_2 \sin(u))\right) du \\ &= (2\pi\sigma^2)^{-1} I_0(r/\sigma^2 \|\mathbf{x}\|) \exp\left(-\frac{r^2 + \|\mathbf{x}\|^2}{2\sigma^2}\right), \end{aligned}$$

where we used

$$\begin{aligned} \left\| \begin{pmatrix} r \cos(u) - x_1 \\ r \sin(u) - x_2 \end{pmatrix} \right\|^2 &= r^2(\cos^2(u) + \sin^2(u)) - 2r(x_1 \cos(u) + x_2 \sin(u)) + x_1^2 + x_2^2 \\ &= r^2 - 2r(x_1 \cos(u) + x_2 \sin(u)) + \|\mathbf{x}\|^2 \end{aligned}$$

and

$$\int_0^{2\pi} \exp\left(t(x_1 \cos(u) + x_2 \sin(u))\right) du = 2\pi I_0(t\|\mathbf{x}\|),$$

with  $I_0$  being the modified Bessel function of the first kind with parameter 0. In general, the modified Bessel function of the first kind with parameter  $\nu \in \mathbb{Z}$  can be written as

$$I_\nu(t) = (t/2)^\nu \sum_{m=0}^{\infty} \frac{(t^2/4)^m}{m!(m+\nu)!}.$$

The derivative of  $I_0$  has the following representation:

$$I'_0(t) = t/2 \sum_{m=1}^{\infty} \frac{m(t^2/4)^{m-1}}{(m!)^2} = t/2 \sum_{m=0}^{\infty} \frac{(t^2/4)^m}{m!(m+1)!} = I_1(t).$$

**Lemma A.1** (Theorem 1 in Simpson and Spector (1984)). *Let be  $\nu(t) := tI_0(t)/I_1(t)$  for  $t > 0$ , then  $\nu(t)$  is strictly increasing and convex with*

$$\nu(0+) = 2, \quad \nu'(0+) = 0 \quad \text{and} \quad \nu''(0+) = \frac{1}{3}.$$

**Lemma A.2.** *For a rotationally symmetric distribution with probability density function  $f : \mathbb{R}^d \rightarrow \mathbb{R}$ ;  $f(\mathbf{x}) = g(\|\mathbf{x}\|)$  for some function  $g : \mathbb{R}_{\geq 0} \rightarrow \mathbb{R}_{\geq 0}$ ,  $g'(0+) = 0$  we have*

$$\text{Ridge}_{d-1}(f) = \{\mathbf{x} \in \mathbb{R}^d : g'(\|\mathbf{x}\|) = 0, g''(\|\mathbf{x}\|) < 0\}.$$

*Proof.* It is  $\mathbf{0} \in \text{Ridge}(f)$  if, and only if,  $g''(0) < 0$ . These, we will assume that  $\mathbf{x} \neq \mathbf{0}$  in the remainder of this proof. It is

$$\begin{aligned} Df(\mathbf{x}) &= g'(\|\mathbf{x}\|) \frac{\mathbf{x}}{\|\mathbf{x}\|}, \\ D^2f(\mathbf{x}) &= g''(\|\mathbf{x}\|) \left( \frac{\mathbf{x}}{\|\mathbf{x}\|} \right) \left( \frac{\mathbf{x}}{\|\mathbf{x}\|} \right)^\top + \frac{g'(\|\mathbf{x}\|)}{\|\mathbf{x}\|} \left( \mathbf{I}_2 - \left( \frac{\mathbf{x}}{\|\mathbf{x}\|} \right) \left( \frac{\mathbf{x}}{\|\mathbf{x}\|} \right)^\top \right), \end{aligned}$$

because

$$\frac{\partial}{\partial x_i} \|\mathbf{x}\| = \frac{1}{2\sqrt{x_1^2 + \dots + x_d^2}} 2x_i = \frac{x_i}{\|\mathbf{x}\|}.$$

Let  $\mathbf{v}_1 := \mathbf{x}/\|\mathbf{x}\|$ , for all vectors  $\mathbf{v} \in \mathbb{R}^d$  with  $\mathbf{v}_1^\top \mathbf{v} = 0$  it holds

$$D^2f(\mathbf{x})\mathbf{v} = \mathbf{0} = 0\mathbf{v}.$$

Hence the space  $\{\mathbf{v} \in \mathbb{R}^d : \mathbf{v}_1^\top \mathbf{v} = 0\} \subset \text{kern}(D^2f(\mathbf{x}))$  and

$$D^2f(\mathbf{x})\mathbf{v}_1 = g''(\|\mathbf{x}\|)\mathbf{v}_1.$$

So, the eigenvalues of  $D^2f(\mathbf{x})$  are  $g''(\|\mathbf{x}\|)$  with multiplicity 1 and 0 with multiplicity  $d - 1$  and  $\mathbf{x} \in \text{Ridge}_{d-1}(f)$  if, and only if,

$$Df(\mathbf{x})^\top \mathbf{v}_1 = g'(\|\mathbf{x}\|)\mathbf{v}_1^\top \mathbf{v}_1 = g'(\|\mathbf{x}\|) = 0 \quad \text{and} \quad g''(\|\mathbf{x}\|) < 0.$$

□

The distribution of the circle data is rotationally symmetric. Indeed,  $f(\mathbf{x}) = g(\|\mathbf{x}\|)$  with

$$\begin{aligned} g(t) &= (2\pi\sigma^2)^{-1} I_0(r/\sigma^2 \cdot t) \exp\left(-\frac{r^2 + t^2}{2\sigma^2}\right), \\ g'(t) &= (2\pi\sigma^2)^{-1} (r/\sigma^2 \cdot I_1(r/\sigma^2 \cdot t) - t/\sigma^2 \cdot I_0(r/\sigma^2 \cdot t)) \exp\left(-\frac{r^2 + t^2}{2\sigma^2}\right). \end{aligned}$$

Denote  $\alpha := r/\sigma^2 > 0$ ,  $t = \|\mathbf{x}\|$ . The following statements are equivalent:

$$\begin{aligned} g'(t) &= 0 \\ \alpha I_1(\alpha t) - t/\sigma^2 \cdot I_0(\alpha t) &= 0 \\ \frac{t}{\sigma^2 \alpha} \frac{I_0(\alpha t)}{I_1(\alpha t)} &= 1 & \text{or } t = 0 \\ \nu(\alpha t) = \alpha t \frac{I_0(\alpha t)}{I_1(\alpha t)} &= \sigma^2 \alpha^2 = \frac{r^2}{\sigma^2} & \text{or } t = 0. \end{aligned}$$

By Lemma A.1 we have  $t = 0$  if  $r/\sigma \leq \sqrt{2}$  and  $t > 0$  if  $r/\sigma > \sqrt{2}$ . The solution is unique and can be calculated by bisection.

## A.2 Matrix Analysis

We state some notation and two results from matrix analysis which will be used later on. References are Bhatia (1997) and Yu et al. (2015).

**Theorem A.3** (Weyl's Inequality; Theorem III.2.1 in Bhatia (1997)). *Let  $\mathbf{A}, \mathbf{B}$  be symmetric  $d \times d$  matrices. Then,*

$$\begin{aligned}\lambda_j(\mathbf{A} + \mathbf{B}) &\geq \lambda_i(\mathbf{A}) + \lambda_{j-i+1}(\mathbf{B}) \quad \text{for } 1 \leq i \leq j, \\ \lambda_j(\mathbf{A} + \mathbf{B}) &\leq \lambda_i(\mathbf{A}) + \lambda_{j-i+d}(\mathbf{B}) \quad \text{for } j \leq i \leq d.\end{aligned}$$

Consequently, for each  $1 \leq j \leq d$ ,

$$\lambda_j(\mathbf{A}) + \lambda_d(\mathbf{B}) \leq \lambda_j(\mathbf{A} + \mathbf{B}) \leq \lambda_j(\mathbf{A}) + \lambda_1(\mathbf{B}).$$

**Theorem A.4** (Davis-Kahan  $\sin \Theta$  Theorem: Theorem VII.3.4 in Bhatia (1997), Theorem 1 in Yu et al. (2015)). *Let  $\mathbf{A}, \mathbf{B}$  be symmetric  $d \times d$  matrices and  $1 \leq s < d$  such that  $\delta := \lambda_s(\mathbf{A}) - \lambda_{s+1}(\mathbf{B}) > 0$ . Then,*

$$\begin{aligned}\frac{\|\mathbf{V}_\perp(\mathbf{A})\mathbf{V}_\perp(\mathbf{A})^\top - \mathbf{V}_\perp(\mathbf{B})\mathbf{V}_\perp(\mathbf{B})^\top\|_F}{\sqrt{2}} &= \|\sin \Theta(\mathbf{V}_\perp(\mathbf{A}), \mathbf{V}_\perp(\mathbf{B}))\|_F \\ &= \|\mathbf{V}_\perp(\mathbf{A})\mathbf{V}_\perp(\mathbf{A})^\top \mathbf{V}_\parallel(\mathbf{B})\mathbf{V}_\parallel(\mathbf{B})^\top\|_F \leq \frac{\|\mathbf{A} - \mathbf{B}\|_F}{\delta},\end{aligned}$$

where  $\Theta(\mathbf{V}_\perp(\mathbf{A}), \mathbf{V}_\perp(\mathbf{B})) \in \mathbb{R}^{d \times d}$  is a diagonal matrix with the vector  $(\cos^{-1}(\sigma_1), \dots, \cos^{-1}(\sigma_d))^\top$ , with  $\sigma_1 \geq \dots \geq \sigma_d \geq 0$  being the singular values of  $\mathbf{V}_\perp(\mathbf{A})^\top \mathbf{V}_\perp(\mathbf{B})$ , on the diagonal. The function  $\sin \Theta(\mathbf{V}_\perp(\mathbf{A}), \mathbf{V}_\perp(\mathbf{B}))$  is defined entry-wise; see Yu et al. (2015).

The first two equalities follow from the definition of the *angle operator* and Exercise VII.1.11 in Bhatia (1997).

## B Proofs

In the following proofs we will suppress the argument  $\mathbf{x}$ .

### B.1 Ridges

**Proof of Theorem 1.6.** We write

$$\boldsymbol{\Sigma}_h = \tilde{\boldsymbol{\Sigma}}_h + \mathbf{M}_h,$$

where

$$\tilde{\boldsymbol{\Sigma}}_h := h^2 \mathbf{I}_d + h^4 D^2 \ell = \mathbf{V}(D^2 \ell) (h^2 \mathbf{I}_d + h^4 \boldsymbol{\Lambda}(D^2 \ell)) \mathbf{V}(D^2 \ell)^\top$$

and

$$\mathbf{M}_h := \boldsymbol{\Sigma}_h - \tilde{\boldsymbol{\Sigma}}_h \quad \text{with} \quad \|\mathbf{M}_h\|_F = \|\boldsymbol{\Lambda}(\mathbf{M}_h)\|_F = o(h^4),$$

by Lemma 1.5. It is

$$\boldsymbol{\Lambda}(\tilde{\boldsymbol{\Sigma}}_h) = h^2 \mathbf{I}_d + h^4 \boldsymbol{\Lambda}(D^2 \ell) \quad \text{and} \quad \mathbf{V}(\tilde{\boldsymbol{\Sigma}}_h) = \mathbf{V}(D^2 \ell).$$

By Weyl's inequality is

$$\lambda_s(\boldsymbol{\Sigma}_h) - \lambda_{s+1}(\tilde{\boldsymbol{\Sigma}}_h) \geq \lambda_s(\tilde{\boldsymbol{\Sigma}}_h) + \lambda_d(\mathbf{M}_h) - \lambda_{s+1}(\tilde{\boldsymbol{\Sigma}}_h) = h^4 \delta + \lambda_d(\mathbf{M}_h) \geq h^4 2^{-1} \delta$$



for  $h$  sufficiently small to achieve  $\lambda_d(\mathbf{M}_h) \geq -h^4 2^{-1} \delta$ , where we used

$$\delta = \lambda_s(D^2 \ell) - \lambda_{s+1}(D^2 \ell) = h^{-4} (\lambda_s(\tilde{\Sigma}_h) - \lambda_{s+1}(\tilde{\Sigma}_h)).$$

By the Davis-Kahan  $\sin \Theta$  Theorem is then

$$\text{dist}(\mathbf{V}_\perp(\Sigma_h), D^2 \ell) \leq \frac{\|\Sigma_h - \tilde{\Sigma}_h\|_F}{h^4 \delta / \sqrt{2}} = \frac{\sqrt{2} \|\mathbf{M}_h\|_F}{h^4 \delta} \rightarrow 0 \quad \text{as } h \rightarrow 0.$$

□

**Proof of Theorem 1.7.** Let  $\mathbf{V}_\perp := \mathbf{V}_\perp(D^2 f(\mathbf{x}))$  and  $\mathbf{V} := \mathbf{V}(D^2 f(\mathbf{x}))$ . The gradient and Hessian matrix of  $\mathbf{z}'' \mapsto \ell(\mathbf{x} + \mathbf{V}_\perp \mathbf{z}'')$  are

$$D(\ell(\mathbf{x} + \mathbf{V}_\perp \mathbf{z}'')) = \mathbf{V}_\perp^\top D\ell(\mathbf{x} + \mathbf{V}_\perp \mathbf{z}'')$$

and

$$D^2(\ell(\mathbf{x} + \mathbf{V}_\perp \mathbf{z}'')) = \mathbf{V}_\perp^\top D^2 \ell(\mathbf{x} + \mathbf{V}_\perp \mathbf{z}'') \mathbf{V}_\perp,$$

respectively, with

$$D\ell(\mathbf{y}) = f(\mathbf{y})^{-1} Df(\mathbf{y}) \quad \text{and} \quad D^2 \ell(\mathbf{y}) = f(\mathbf{y})^{-1} D^2 f(\mathbf{y}) - f(\mathbf{y})^{-2} Df(\mathbf{y}) Df(\mathbf{y})^\top.$$

The matrix  $D^2(\ell(\mathbf{x} + \mathbf{V}_\perp \mathbf{z}''))$  is negative definite, whenever  $\mathbf{u}^\top D^2 f(\mathbf{x} + \mathbf{V}_\perp \mathbf{z}'') \mathbf{u} < 0$  for any unit vector in the column space of  $\mathbf{V}_\perp$ . We have

$$\begin{aligned} \mathbf{u}^\top D^2 f(\mathbf{x} + \mathbf{V}_\perp \mathbf{z}'') \mathbf{u} &= \mathbf{u}^\top D^2 f(\mathbf{x}) \mathbf{u} + \mathbf{u}^\top (D^2 f(\mathbf{x} + \mathbf{V}_\perp \mathbf{z}'') - D^2 f(\mathbf{x})) \mathbf{u} \\ &\leq \mathbf{u}^\top \mathbf{V} \mathbf{A} (D^2 f(\mathbf{x})) \mathbf{V}^\top \mathbf{u} + \mathbf{u}^\top (D^2 f(\mathbf{x} + \mathbf{V}_\perp \mathbf{z}'') - D^2 f(\mathbf{x})) \mathbf{u} \\ &\leq \mathbf{u}^\top \mathbf{V}_\perp \text{diag}(\lambda_{s+1}(D^2 f(\mathbf{x})), \dots, \lambda_d(D^2 f(\mathbf{x}))) \mathbf{V}_\perp^\top \mathbf{u} \\ &\quad + |\mathbf{u}^\top (D^2 f(\mathbf{x} + \mathbf{V}_\perp \mathbf{z}'') - D^2 f(\mathbf{x})) \mathbf{u}| \\ &\leq \sum_{j=s+1}^d \lambda_j(D^2 f(\mathbf{x})) (\mathbf{u}^\top \mathbf{v}_j(D^2 f(\mathbf{x})))^2 \\ &\quad + \sup_{\mathbf{v} \in \mathbb{S}^{d-1}} |\mathbf{u}^\top (D^2 f(\mathbf{x} + \mathbf{V}_\perp \mathbf{z}'') - D^2 f(\mathbf{x})) \mathbf{u}| \\ &\leq \lambda_{s+1}(D^2 f(\mathbf{x})) + \|D^2 f(\mathbf{x} + \mathbf{V}_\perp \mathbf{z}'') - D^2 f(\mathbf{x})\|_F, \end{aligned}$$

where we used  $\mathbf{V}_\perp \mathbf{V}_\perp^\top \mathbf{u} = \mathbf{u}$  and the fact, that  $\sup_{\mathbf{v} \in \mathbb{S}^{d-1}} |\mathbf{v}^\top \mathbf{A} \mathbf{v}| \leq \|\mathbf{A}\|_F$  for any symmetric matrix  $\mathbf{A} \in \mathbb{R}^{d \times d}$ . By continuity of  $D^2 f$ , there exists  $\varepsilon > 0$  such that  $\|D^2 f(\mathbf{x} + \mathbf{V}_\perp \mathbf{z}'') - D^2 f(\mathbf{x})\|_F < |\lambda_{s+1}(D^2 f(\mathbf{x}))|$  for any  $\mathbf{z}'' \in \mathbb{R}^{d-s}$  with  $\|\mathbf{z}''\| < \varepsilon$  and so  $\mathbf{u}^\top D^2 f(\mathbf{x} + \mathbf{V}_\perp \mathbf{z}'') \mathbf{u} < 0$ , because  $\lambda_{s+1}(D^2 f(\mathbf{x})) < 0$ .

The function  $\mathbf{z}'' \mapsto f(\mathbf{x} + \mathbf{V}_\perp \mathbf{z}'')$  has a mode at  $\mathbf{0}_{d-s}$ , because

$$D(\ell(\mathbf{x} + \mathbf{V}_\perp \mathbf{z}'')) \Big|_{\mathbf{z}'' = \mathbf{0}} = \mathbf{V}_\perp^\top D\ell(\mathbf{x}) = f(\mathbf{x})^{-1} \mathbf{V}_\perp^\top Df(\mathbf{x}) = 0.$$

□

**Proof of Theorem 1.8.** By Theorem 1.7 we know, that the function  $t \mapsto f(\mathbf{x} + t\mathbf{u})$  has a mode at  $t = 0$  for any  $\mathbf{u}$  in the column space of  $\mathbf{V}_\perp(D^2 \ell(\mathbf{x}))$ . Therefore, the directional derivatives in directions  $\mathbf{v}_j := \mathbf{v}_j(D^2 \ell(\mathbf{x}))$  for  $s+1 \leq j \leq d$  are equal to zero:

$$0 = \frac{d}{dt} \Big|_{t=0} \ell(\mathbf{x} + t\mathbf{v}_j(D^2 \ell(\mathbf{x}))) = \mathbf{v}_j(D^2 \ell(\mathbf{x}))^\top D\ell(\mathbf{x}),$$

whence  $\mathbf{V}_\perp(D^2\ell(\mathbf{x}))^\top D\ell(\mathbf{x}) = \mathbf{0}$ . Furthermore, the second directional derivatives are strictly negative. So,

$$0 > \frac{d^2}{dt^2}\ell(\mathbf{x} + t\mathbf{v}_j)\Big|_{t=0} = \mathbf{v}_j^\top D^2\ell(\mathbf{x})\mathbf{v}_j = \sum_{i=1}^d \lambda_i(D^2\ell(\mathbf{x}))\mathbf{v}_j^\top \mathbf{v}_i \mathbf{v}_i^\top \mathbf{v}_j = \lambda_j(D^2\ell(\mathbf{x}))$$

for  $s+1 \leq j \leq d$  □

**Proof of Theorem 1.9.** We write  $K = e^\psi$  for some  $\psi \in \mathcal{C}^2(\text{supp}(K))$  and  $\mathbf{V} := \mathbf{V}(\boldsymbol{\Sigma}_h(\mathbf{x}))$ , then the logarithm of the integrand of  $g_h$  is

$$\log(K(\mathbf{z})f(\mathbf{x} + \mathbf{V}\mathbf{z})) = \psi(\mathbf{z}) + \ell(\mathbf{x} + \mathbf{V}\mathbf{z})$$

and Hessian matrix

$$D^2\psi(\mathbf{z}) + h^2\mathbf{V}^\top D^2\ell(\mathbf{x} + \mathbf{V}\mathbf{z})\mathbf{V}.$$

Because  $D^2\ell$  is bounded by assumption, there exists  $h_o > 0$  such that the Hessian matrix is negative definite for all  $0 < h < h_o$ . □

## B.2 Algorithms

In the following, we will use local moments defined as

$$s_n^\alpha(\mathbf{x}) := \frac{1}{n} \sum_{i=1}^n K_h(h^{-1}(\mathbf{X}_i - \mathbf{x}))h^{-|\alpha|}(\mathbf{X}_i - \mathbf{x})^\alpha \quad \text{for } \alpha \in \mathbb{N}_0^d \quad \text{and} \quad s_n(\mathbf{x}) := s_n^{\mathbf{0}}(\mathbf{x}).$$

**Proof of Theorem 2.1.** Let  $\tilde{L}, m > 0$  and  $M > 1$  be the constants as given in Lemma B.1 and B.2 stated below. Then,

$$\begin{aligned} \|\hat{\boldsymbol{\Sigma}}_{n,h}(\mathbf{x}) - \hat{\boldsymbol{\Sigma}}_{n,h}(\mathbf{y})\|_F^2 &= \sum_{1 \leq i,j \leq d} \left( \frac{s_n^{\mathbf{e}_i + \mathbf{e}_j}(\mathbf{x})}{s_n(\mathbf{x})} - \frac{s_n^{\mathbf{e}_i + \mathbf{e}_j}(\mathbf{y})}{s_n(\mathbf{y})} + \frac{s_n^{\mathbf{e}_i}(\mathbf{x})s_n^{\mathbf{e}_j}(\mathbf{x})}{s_n(\mathbf{y})^2} - \frac{s_n^{\mathbf{e}_i}(\mathbf{y})s_n^{\mathbf{e}_j}(\mathbf{x})}{s_n(\mathbf{y})^2} \right)^2 \\ &\leq 2 \sum_{1 \leq i,j \leq d} \left( \left( \frac{s_n^{\mathbf{e}_i + \mathbf{e}_j}(\mathbf{x})}{s_n(\mathbf{x})} - \frac{s_n^{\mathbf{e}_i + \mathbf{e}_j}(\mathbf{y})}{s_n(\mathbf{y})} \right)^2 + \left( \frac{s_n^{\mathbf{e}_i}(\mathbf{x})s_n^{\mathbf{e}_j}(\mathbf{x})}{s_n(\mathbf{x})^2} - \frac{s_n^{\mathbf{e}_i}(\mathbf{y})s_n^{\mathbf{e}_j}(\mathbf{y})}{s_n(\mathbf{y})^2} \right)^2 \right) \\ &\leq 2 \sum_{1 \leq i,j \leq d} \left( \left( \frac{2M\tilde{L}}{m^2} \right)^2 \|\mathbf{x} - \mathbf{y}\|^2 + \left( \frac{4M^2\tilde{L}}{m^2} \right)^2 \|\mathbf{x} - \mathbf{y}\|^2 \right) \\ &\leq 2d^2 \left( \frac{4M^2\tilde{L}}{m^2} \right)^2 \|\mathbf{x} - \mathbf{y}\|^2, \end{aligned}$$

This shows,

$$\|\hat{\boldsymbol{\Sigma}}_{n,h}(\mathbf{x}) - \hat{\boldsymbol{\Sigma}}_{n,h}(\mathbf{y})\|_F \leq \frac{4dM\sqrt{\tilde{L}}}{m^2} \|\mathbf{x} - \mathbf{y}\|. \quad \square$$

**Lemma B.1.** For a sample  $\mathcal{X} = \{\mathbf{X}_1, \dots, \mathbf{X}_n\}$ , fixed  $h$  and a Kernel  $K$  with  $\sup_{|\gamma|=1} \|K^{(\gamma)}\|_\infty < \infty$ , the local sample moments up to order 2 are Lipschitz continuous on the convex hull of the sample, i.e. there exists  $\tilde{L} > 0$ , such that

$$|s_n^\alpha(\mathbf{x}) - s_n^\alpha(\mathbf{y})| \leq \tilde{L} \|\mathbf{x} - \mathbf{y}\| \quad \text{for } \mathbf{x}, \mathbf{y} \in \text{conv}(\mathbf{X}_1, \dots, \mathbf{X}_n) \quad \text{for all } \alpha \in \mathbb{N}_0^d \text{ with } |\alpha| \leq 2$$

*Proof.* It is

$$\begin{aligned}
s_n^\alpha(\mathbf{y}) &= \frac{1}{n} \sum_{i=1}^n K_h(\mathbf{X}_i - \mathbf{y})(\mathbf{X}_i - \mathbf{x} + \mathbf{x} - \mathbf{y})^\alpha \\
&= \frac{1}{n} \sum_{i=1}^n K_h(\mathbf{X}_i - \mathbf{y}) \sum_{\gamma \leq \alpha} \binom{\alpha}{\gamma} (\mathbf{x} - \mathbf{y})^\gamma (\mathbf{X}_i - \mathbf{x})^{\alpha - \gamma} \\
&= s_n^\alpha(\mathbf{x}) + \frac{1}{n} \sum_{i=1}^n K_h(\mathbf{X}_i - \mathbf{y}) \sum_{\substack{|\gamma| \geq 1 \\ \gamma \leq \alpha}} \binom{\alpha}{\gamma} (\mathbf{x} - \mathbf{y})^\gamma (\mathbf{X}_i - \mathbf{x})^{\alpha - \gamma} \tag{4}
\end{aligned}$$

$$+ \frac{1}{n} \sum_{i=1}^n (\mathbf{X}_i - \mathbf{x})^\alpha (K_h(\mathbf{X}_i - \mathbf{y}) - K_h(\mathbf{X}_i - \mathbf{x})), \tag{5}$$

where

$$\binom{\alpha}{\gamma} := \frac{\alpha!}{\gamma!(\alpha - \gamma)!}$$

and  $\gamma \leq \alpha$  is to be understood component-wise. The absolute value of (4) can then be bounded by

$$\|K\|_\infty \|\mathbf{x} - \mathbf{y}\| \sum_{\substack{|\gamma| \geq 1 \\ \gamma \leq \alpha}} \binom{\alpha}{\gamma} \text{diam}(\mathcal{X})^{|\gamma|-1} \leq 3\|K\|_\infty \max(\text{diam}(\mathcal{X}), 1) \|\mathbf{x} - \mathbf{y}\|,$$

because

$$\sum_{\substack{|\gamma| \geq 1 \\ \gamma \leq \alpha}} \binom{\alpha}{\gamma} = \begin{cases} 1 & \text{for } |\alpha| = 1, \\ 3 & \text{for } |\alpha| = 2. \end{cases}$$

The absolute value of (5) is bounded by

$$\begin{aligned}
&\max(\text{diam}(\mathcal{X}), 1)^{|\alpha|} h^{-d} |K(h^{-1}(\mathbf{X}_i - \mathbf{y})) - K(h^{-1}(\mathbf{X}_i - \mathbf{x}))| \\
&\leq \max(\text{diam}(\mathcal{X}), 1)^{|\alpha|} h^{-d-1} \sup_{|\gamma|=1} \|K^{(\gamma)}\|_\infty \|\mathbf{x} - \mathbf{y}\|.
\end{aligned}$$

Hence,

$$|s_n^\alpha(\mathbf{y}) - s_n^\alpha(\mathbf{x})| \leq \max(\text{diam}(\mathcal{X}), 1)^2 \sup_{|\gamma|=1} \|K^{(\gamma)}\|_\infty (3 + h^{-2}) \|\mathbf{y} - \mathbf{x}\|,$$

for any  $\alpha$  with  $0 \leq |\alpha| \leq 2$ . □

**Lemma B.2.** *The quotient  $s_n^\alpha(\mathbf{x})/s_n(\mathbf{x})$  is Lipschitz continuous, whenever there exists  $0 < \tau \leq s_n(\mathbf{x})$  for  $\mathbf{x} \in \text{conv}(\mathbf{X}_1, \dots, \mathbf{X}_n)$ .*

*Proof.* Let

$$M := \max_{\substack{0 \leq |\alpha| \leq 2 \\ \mathbf{z} \in \text{conv}(\mathcal{X})}} s_n^\alpha(\mathbf{z}),$$

then

$$\begin{aligned}
\left| \frac{s_n^\alpha(\mathbf{y})}{s_n(\mathbf{y})} - \frac{s_n^\alpha(\mathbf{x})}{s_n(\mathbf{x})} \right| &\leq \frac{1}{m^2} |s_n^\alpha(\mathbf{y})s_n(\mathbf{x}) - s_n^\alpha(\mathbf{x})s_n(\mathbf{y})| \\
&\leq \frac{1}{m^2} (|s_n^\alpha(\mathbf{y})s_n(\mathbf{x}) - s_n^\alpha(\mathbf{x})s_n(\mathbf{x})| + |s_n^\alpha(\mathbf{x})s_n(\mathbf{x}) - s_n^\alpha(\mathbf{x})s_n(\mathbf{y})|) \\
&\leq \frac{1}{m^2} (|s_n(\mathbf{x})| \cdot |s_n^\alpha(\mathbf{y}) - s_n^\alpha(\mathbf{x})| + |s_n^\alpha(\mathbf{x})| \cdot |s_n(\mathbf{x}) - s_n(\mathbf{y})|) \\
&\leq \frac{2M\tilde{L}}{m^2} \|\mathbf{x} - \mathbf{y}\|,
\end{aligned}$$

for any  $\mathbf{x}, \mathbf{y} \in \text{conv}(\mathcal{X})$ . □

**Smoothed ridge.** The following calculations are useful to find the unique mode of  $\hat{g}^*$  via the Newton method. We have

$$\hat{g}^*(y) = \sum_{j=2}^m \hat{g}_{j-1} \int_{x_{j-1}}^{x_j} \exp(\hat{s}_j(t - x_{j-1})) \phi_\gamma(y - t) dt = \sum_{j=2}^m \hat{f}_{j-1} q_\gamma(y, \hat{s}_j, x_{j-1}, x_j),$$

where  $x_1 < x_2 < \dots < x_m$  denote the knots of the log-density estimator  $\hat{g}$ ,  $\hat{g}_{j-1} := \hat{g}(x_{j-1})$  and  $\hat{s}_j := \frac{\log(\hat{f}_j) - \log(\hat{f}_{j-1})}{x_j - x_{j-1}}$  for  $2 \leq j \leq m$ . The auxiliary function  $q_\gamma$  is

$$q_\gamma(x, a, u, v) := \int_u^v e^{a(x-u)} \phi_\gamma(x - y) dt = e^{a(x-u) + a^2\gamma^2/2} \left( \Phi\left(\frac{v-x-a\gamma^2}{\gamma}\right) - \Phi\left(\frac{u-x-a\gamma^2}{\gamma}\right) \right),$$

$$\begin{aligned}
q'_\gamma(x, a, u, v) &= a q_\gamma(x, a, u, v) + e^{a(x-u) + a^2\gamma^2/2} \gamma^{-1} \left( \phi\left(\frac{u-x-a\gamma^2}{\gamma}\right) - \phi\left(\frac{v-x-a\gamma^2}{\gamma}\right) \right) \\
&= a q_\gamma(x, a, u, v) + \frac{\gamma^{-1}}{\sqrt{2\pi}} \left( e^{a(x-u) + a^2\gamma^2/2 - \ell^2/2} - e^{a(x-u) + a^2\gamma^2/2 - r^2/2} \right)
\end{aligned}$$

and

$$\begin{aligned}
q''_\gamma(x, a, u, v) &= 2a q'_\gamma(x, a, u, v) - a^2 q_\gamma(x, a, u, v) + e^{a(x-u) + a^2\gamma^2/2} \gamma^{-2} \left( \phi'\left(\frac{v-x-a\gamma^2}{\gamma}\right) - \phi'\left(\frac{u-x-a\gamma^2}{\gamma}\right) \right) \\
&= 2a q'_\gamma(x, a, u, v) - a^2 q_\gamma(x, a, u, v) \frac{\gamma^{-2}}{\sqrt{2\pi}} \left( \ell e^{a(x-u) + a^2\gamma^2/2 - \ell^2/2} - r e^{a(x-u) + a^2\gamma^2/2 - r^2/2} \right),
\end{aligned}$$

where  $\phi$  and  $\Phi$  is the density and distribution function of a standard normal, respectively, and

$$r := \frac{v-x-a\gamma^2}{\gamma} \quad \text{and} \quad \ell := \frac{u-x-a\gamma^2}{\gamma}.$$

Note that

$$\phi'\left(\frac{v-x-a\gamma^2}{\gamma}\right) - \phi'\left(\frac{u-x-a\gamma^2}{\gamma}\right) = \frac{u-x-a\gamma^2}{\gamma} \phi\left(\frac{u-x-a\gamma^2}{\gamma}\right) - \frac{v-x-a\gamma^2}{\gamma} \phi\left(\frac{v-x-a\gamma^2}{\gamma}\right).$$

Thus,

$$\begin{aligned}\widehat{f}^*(x) &= \sum_{j=2}^m \widehat{f}_{j-1} q_{\gamma}(x, \widehat{s}_j, x_{j-1}, x_j), \\ \widehat{f}^*(x)' &= \sum_{j=2}^m \widehat{f}_{j-1} q'_{\gamma}(x, \widehat{s}_j, x_{j-1}, x_j), \\ \widehat{f}^*(x)'' &= \sum_{j=2}^m \widehat{f}_{j-1} q''_{\gamma}(x, \widehat{s}_j, x_{j-1}, x_j).\end{aligned}$$